Current Research in Microbial Sciences 9 (2025) 100462

Contents lists available at ScienceDirect

Current Research in Microbial Sciences

journal homepage: www.sciencedirect.com/journal/current-research-in-microbial-sciences

Enhancing diagnostic efficiency of pyrazinamide resistance in *Mycobacterium tuberculosis* via modified MGIT assay and genotypic correlation

Ananthi Rajendran [a], Ahmed Kabir Refaya [a], Balaji Subramanyam [b], Ramesh Karunaianantham [c], Dhandapani RaviKumar [b], Hemalatha Haribabu [c], Radha Gopalaswamy [b], Radhika Golla [b], Vadivel Senthildevi [b], Narayanan Sivaramakrishnan Gomathi [b], Sivakumar Shanmugam [b], Kannan Palaniyandi [a,*]

[a] Department of Immunology, ICMR-National Institute for Research in Tuberculosis, Chennai, India
[b] Department of Bacteriology, ICMR-National Institute for Research in Tuberculosis, Chennai, India
[c] Department of Virology & Biotechnology, ICMR-National Institute for Research in Tuberculosis, Chennai, India

ARTICLE INFO

Keywords:
Pyrazinamide resistance
Drug susceptibility
Novel mutation
Mycobacterium tuberculosis

ABSTRACT

Pyrazinamide (PZA) plays a crucial role in the treatment of both active and latent tuberculosis, particularly in regimens designed to treat drug-resistant TB. However, diagnosing resistance to PZA poses challenges for managing TB, highlighting the need for accurate detection methods. This study aims to address the challenges in detecting PZA resistance by modifying the standard MGIT960 PZA drug susceptibility testing method by optimizing the inoculum dilution. Briefly, three MGIT DST versions were evaluated: the standard method, the reduced inoculum (RI) method employing a 1:20 inoculum dilution and the sparse dilution (SD) method using a 1:50 dilution of the inoculum for growth control tube, while the undiluted MGIT positive culture was used for the PZA test tube. The SD MGIT DST approach minimized the number of false-resistant PZA results to (31/401) 7.7 % against 27 % by standard MGIT DST and 11.7 % by RI MGIT DST approach, thereby reducing the false-positivity rate by 19.3 %. Targeted sequencing of *pncA* gene identified mutations in only 14/401 isolates (3.5 %). Whole genome sequencing (WGS) of the 31 phenotypically resistant isolates identified resistance -associated mutations in *pncA* gene (45 %), *panD* (9.6 %), *mas* (12.9 %), *glpK* (3.2 %), and *lprG* (3.2 %), and others efflux associated genes like *Rv1258c* (3.2 %), *Rv0191c* (3.2 %), and *Rv3008* (6.45 %), except for 4 isolates, for which no mutations were detected in the target genes. These genes are involved in various resistance mechanisms including cell wall synthesis, metabolic pathways, and drug tolerance, which are essential for PZA efficacy. Notably, new mutations in *glpK* and *mas* were detected in isolates with wild-type *pncA* and were absent in the sensitive isolates. Our study substantiates the improvement of phenotypic testing methods and enhances the detection of PZA resistance even in resource-limited settings and direct research towards improving the diagnostic accuracy in TB drug resistance management.

1. Introduction

Globally, the incidence of multidrug-resistant tuberculosis (MDR-TB) is on the rise, leading to significant treatment failures primarily attributed to resistance against key first-line anti-TB drugs, such as isoniazid and rifampicin (Ahmad et al., 2018; Brust et al., 2016). The World Health Organization (WHO) reported 10.8 million incident cases, 8.2 million new TB cases and 1.25 million deaths in 2023, with India contributing 26 % of the global TB burden, the highest share worldwide. India also holds the highest proportion of MDR-TB cases, accounting for 27 % of global TB cases (WHO, 2024). Among the core components of TB regimens for MDR-TB, pyrazinamide (PZA) plays a crucial role and is used in combination with other TB drugs to shorten TB therapy. However, it is imperative to acknowledge that the patterns of resistance to

* Corresponding author at: Scientist "E," Department of Immunology, ICMR-National Institute for Research in Tuberculosis, #1, Mayor Sathyamoorthy Road, Chetpet, Chennai 600031, India.
E-mail address: palaniyandi.k@icmr.gov.in (K. Palaniyandi).

https://doi.org/10.1016/j.crmicr.2025.100462

Available online 23 August 2025
2666-5174/© 2025 The Authors. Published by Elsevier B.V. This is an open access article under the CC BY-NC-ND license (http://creativecommons.org/licenses/by-nc-nd/4.0/).

PZA are influenced by various factors, including genetic background, prior exposure to anti-TB drugs, and PZA use in TB treatment (Balay et al., 2024; Modlin et al., 2021; Ullah et al., 2016). A systematic review and meta-analysis reported a global prevalence of 29 % for PZA resistance among TB cases, 17 % among the high risk of MDR-TB patients, and 75 % in the MDR-TB patients (Wang et al., 2023). In India, PZA resistance rates of 6.95 % among new TB patients and 8.77 % among previously treated TB patients have been reported (India TB Report 2016). A recent investigation identified PZA resistance as the most prevalent among XDR isolates (68 %; 23/34), followed by pre-XDR (64 %; 756/1178), MDR (31 %; 133/432), and polydrug resistance (13 %; 29/230) (Tamilzhalagan et al., 2025).

The clinical importance of PZA is attributed to its distinctive sterilizing effect on semi-dormant *Mycobacterium tuberculosis* bacilli in acidic environments, making it a critical component of both first-line and MDR-TB treatment regimens (Zhang and Mitchison, 2003). However, PZA resistance in *M. tuberculosis* remains challenging because of the complexity of its resistance mechanisms and limitations of current diagnostic methods (Thuansuwan et al., 2024). The WHO's recommendation on the use of the BD MGIT 960 PZA susceptibility kit with a low pH (World Health Organization, 2018) aligns with the longstanding hypothesis that PZA is active against *M. tuberculosis* only at acidic pH (Mitchison, 1985; Salfinger and Heifets, 1988; Zhang et al., 2003; Zhang and Mitchison, 2003). Nevertheless, a few recent studies have shown that *M. tuberculosis* is also susceptible to PZA at neutral pH, reduced temperature, and alkaline pH, highlighting the complexities surrounding its mechanism and the need for more reliable and universally applicable phenotypic methods (Den Hertog et al., 2016; Peterson et al., 2015; Shi, 2021).

A significant drawback of using acidified media is its inhibition of most clinical strains of *M. tuberculosis* growth at a pH level below 6.0 (Gouzy et al., 2021; Piddington et al., 2000). This impaired growth results in false susceptibility when PZA phenotypic methods are used (Morlock et al., 2017; Piersimoni et al., 2013). Furthermore, slow-growing populations are exposed to PZA in acidic environments, may require multiple bacterial generations to achieve optimal bactericidal effects (Pullan et al., 2016). In our study, we addressed this issue by extending the incubation period to allow ample time for growth under acidic conditions, with the aim of enhancing the precision of PZA susceptibility testing.

Accurate diagnosis of drug resistance in tuberculosis is crucial for effective treatment. Various methods are used to diagnose PZA resistance, including Wayne's assay, MGIT960 drug susceptibility testing (DST), targeted sequencing, and next-generation sequencing (NGS) (Nasiri et al., 2021; Werngren et al., 2021; Rajendran and Palaniyandi, 2022). Wayne's assay, a conventional method, is widely used for detecting PZA resistance, but is limited only to *pncA* mutations, with a reported sensitivity of ~75.6 % and specificity of ~88.7 % (Nasiri et al., 2021). The MGIT 960 system has been reported as a reliable method for phenotypic PZA susceptibility testing (Sharma et al., 2010). However, reports indicate a high false resistance rate of up to 58.2 % due to excessive bacterial inoculum which can raise the medium's pH and result in poor reproducibility (Piersimoni et al., 2013; Werngren et al., 2012). To mitigate this, subsequent studies proposed protocol modifications such as reducing the inoculum size from 0.5 ml to 0.25 ml, decreases the false resistance rates from 26 % to 11 %, compared to the standard MGIT assay (Piersimoni et al., 2013). Further refinements by Morlock et al. (2017) examined two different approaches, where the first method used a 1:25 dilution of the inoculum for the control tube and 1:2.5 for the PZA tube and a second method further reduced the inoculum was to 1:50 and 1:5 dilutions respectively. These methods reduced the false resistant results from 55.2 % in the standard test to 28.8 % and 16 % for the first and second dilutions, respectively (Morlock et al., 2017). However, this approach has used different dilutions of the inoculum for the control and PZA tubes, invoking complexities. Our study builds on these techniques utilized the novel sparse dilution (1:50) approach designed to simplify the protocol, minimize pH fluctuations, and reduce false resistance without requiring different dilution ratios for the control and PZA tubes. This method further reduces the bacillary load, allowing sufficient time for the drug to act while preserving the acidic conditions required for PZA activity, compared to the RI MGIT DST and standard MGIT DST methods.

Implementing molecular methods for detecting PZA resistance is challenging due to heterogeneity in mutations associated with PZA resistance, particularly in the *pncA* gene encoding pyrazinamidase (PZase) (Chang et al., 2011; Karmakar et al., 2020). The performance of *pncA*-based molecular diagnostics is being considered by the WHO, with the inclusion of other genes, such as *panD* and *rpsA*, to improve the detection of PZA resistance (Ramirez-Busby et al., 2017; Thiede et al., 2021). These findings highlight the ongoing efforts to improve the accuracy of diagnosing PZA resistance for better treatment outcomes. Whole genome sequencing (WGS) is a powerful tool that identifies mutations across the entire genome (Nimmo et al., 2019), including genes not traditionally considered in resistance studies. This approach has enabled the discovery of previously unknown or novel mutations associated with resistance, providing a more complete understanding of the genetic mechanisms underlying resistance. Whole genome sequencing has been employed to detect and predict drug resistance in *M. tuberculosis* (Allix-Beguec et al., 2018). It was used as the reference method for defining the resistance and susceptibility profiles of the study isolates. Although phenotypic DST remains the gold standard, the high resolution and predictive accuracy of WGS for known resistance-related mutations have led to its increased acceptance in research settings (Koser et al., 2012). Accordingly, we evaluated the performance of various phenotypic methods in relation to the genotypic classification provided by WGS. Despite increasing recognition of the role of non-*pncA* genes in conferring PZA resistance, there is still a lack of extensive data correlating these mutations with phenotypic resistance profiles. Our study addresses this gap by employing WGS with optimized phenotypic DST to identify novel mutations, particularly in isolates lacking *pncA* mutations and in genes that have not previously been reported to harbor resistance-associated mutations in clinical isolates, contributing to a more comprehensive understanding of the genetic landscape of PZA resistance.

This primary objective of the study seeks to resolve concerns regarding false resistance and overcome challenges in assessing PZA resistance in *M. tuberculosis* by further modifying the reduced inoculum (RI) by Piersimoni et al. who used a lower bacterial load in the growth control (GC) tube and with a sparse dilution (SD) approach, employing an even greater dilution for the GC tube to prolong incubation and enhance test accuracy (Piersimoni et al., 2013). Recognizing that PZA resistance may extend beyond the *pncA* gene and as a secondary objective this study analyzed the genetic makeup of the isolates and explored additional genes contributing to PZA resistance using WGS. Advocating the integration of genotypic methods with standardized testing helps understand resistance mechanisms, contributing to improved diagnostic precision and effective treatment strategies. This study evaluated PZA resistance in presumed drug-resistant *M. tuberculosis* isolates using SD MGIT DST, Wayne's method, targeted sequencing, and WGS seeking correlations between phenotypic outcomes and genotypic assessment to address challenges in detection of emerging drug resistance.

2. Methods

2.1. Isolate selection, phenotypic assays and genotypic sequencing

The samples included in this study were retrieved from archived cultures stored at the National Institute for Research in Tuberculosis (NIRT), Chennai, South India, from 2019 to 2020. These clinical isolates were initially identified as presumptive drug-resistant strains, although the specific phenotypic and genotypic resistance profiles were unknown

at the time of inclusion. The stored cultures were revived in Lowenstein-Jensen (LJ) medium and inoculated into MGIT tubes, the cultures that exhibited positive growth were included, and the cultures that were unable to be revived and cultures that had contamination or mixed mycobacterial growth and non-tuberculous mycobacteria were excluded from the study. All isolates were anonymized prior to analysis, and the study was approved by the institutional ethics committee (NIRT-IEC ID 2019002). A total of 401 isolates were selected for this study using convenience sampling. These isolates were subjected to phenotypic MGIT 960 standard DST, reduced inoculum (RI) MGIT DST, and sparse dilution (SD) MGIT DST methods with 100 µg/ml concentration of PZA (Fig. 1). Additionally, PZase activity by Wayne's method and genotypic methods including targeted and whole genome sequencing were used to determine resistance profile.

2.2. MGIT 960 standard DST method

The phenotypic MGIT 960 method was used to assess the susceptibility of clinical strains to first-line TB drugs, including rifampicin (RIF), isoniazid (INH), and pyrazinamide (PZA). Isolates from preserved cultures were revived and inoculated onto MGIT 7H9 tubes containing 0.8 ml of PANTA supplement. The cultures were then grown until MGIT 960 indicated that the results were positive. For each drug, the DST was performed according to the manufacturer's standard procedure (Becton, Dickinson, and Company) (Siddiqi and Rüsch-Gerdes, 2006). Here, *M. tuberculosis* strain H37Rv was used as a PZA-susceptible control and *M. bovis* BCG was used as a PZA-resistant control (Sharma et al., 2010). For each isolate, three 7 ml 7H9 MGIT tubes were used, one labeled as GC, and the other two as INH and RIF. For the PZA DST, two MGIT PZA tubes were used, one for GC and the other for the PZA drug-containing tube. To each tube, 0.8 ml MGIT SIRE/PZA supplement was added, followed by 0.1 ml of the respective drug in the corresponding tubes. The inoculum prepared from positive MGIT tubes, and two sterile 15 mL Falcon tubes were labeled for 1:10 and 1:100 dilution. Positive MGIT cultures on days 1–2 was vortexed and allowed to settle. Then, 0.1 ml of the culture supernatant with 9.9 ml of saline was transferred to 1:100 dilution tube, vortexed, and allowed to settle for 15 min. From this 1:100 diluted suspension, 0.5 ml was inoculated into GC tubes for INH and RIF. Simultaneously, 0.5 ml of the positive MGIT culture with 4.5 ml of sterile saline was added to the 1:10 tube, vortexed and stand for 15 min. The resulting suspension, 0.5 ml was transferred to the PZA-GC tube. All tubes were gently tilted 3–4 times to ensure mixing. If the MGIT cultures were positive on days 3–5, 1 ml was added to 4 ml of saline tube labeled as "Neat" (1:5 dilution). Suspensions of 1:10 and 1:100 were prepared from this "Neat" using sterile saline, following the same procedure described above. The DST results showed that the growth unit (GU) value in the GC tube must reach a minimum of 400 to confirm valid culture growth. For drug-containing tubes, a GU value above 100 indicates resistance to the respective drug, while a GU value below 100 indicates drug susceptible based on the WHO guidelines for standard MGIT DST (World Health Organization, 2018).

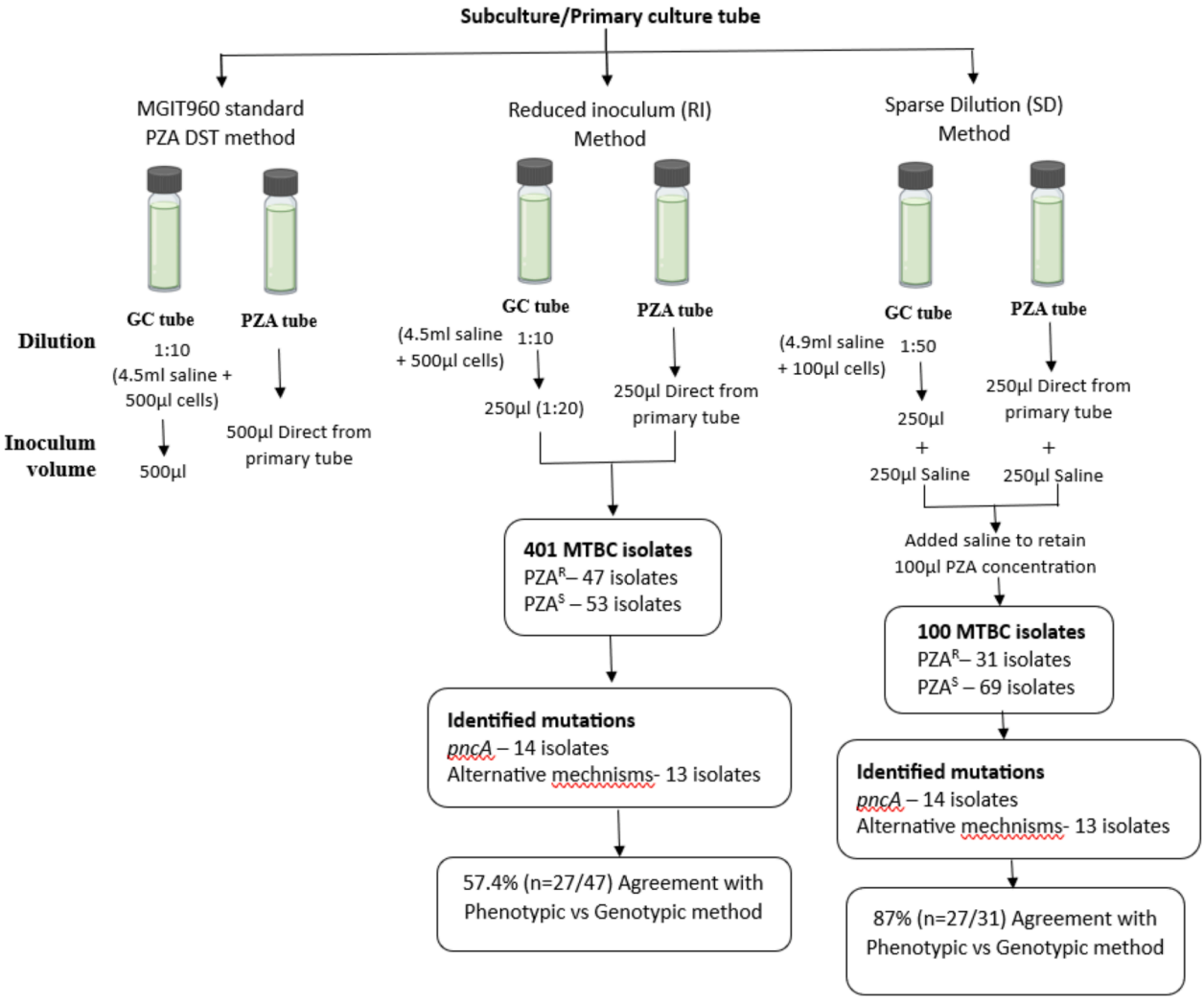

Fig. 1. MGIT PZA susceptibility testing performed using three different protocols to assess phenotypic resistance in *M. tuberculosis* isolates.

2.3. Reduced inoculum (RI) MGIT DST method

The reduced inoculum for PZA susceptibility testing was carried out in accordance with the procedure standardized by Piersimoni et al. (2013). For each isolate, the inoculum was prepared from MGIT-positive cultures (1–5 days positive), following the MGIT protocol. The main modification consisted of reducing the inoculum volume from 0.5 mL to 0.25 mL for both the GC and PZA test tube. A 1:10 dilution of the culture suspension was prepared, and 0.25 mL of this diluted suspension was added to the GC tube. This resulted 20-fold (1:20) reduction of bacterial load compared to the standard MGIT method, and a 2-fold reduction in the PZA tube. The remainder of the protocol remains unchanged. Based on previous investigations, this modification was performed to reduce false PZA resistance and to ensure susceptibility evaluation (Piersimoni et al., 2013).

2.4. Sparse dilution (SD) MGIT DST method

In the SD MGIT DST method, an inoculum dilution of 1:50 was prepared from MGIT-positive tubes (1–5 days positive). The tubes were vortexed for homogenization and the clumps allowed to settle for 15 min. From the upper portion, 100 μL of the culture suspension was transferred into 4.9 mL of sterile saline for a 1:50 dilution. Subsequently, 0.25 mL of this dilution was inoculated into the GC tube, followed by the addition of 250 μL of sterile saline. Similarly, 250 μL of the undiluted culture suspension and 250 μL of sterile saline were added to the PZA test tube to achieve a total volume of 500 μL (Fig. 1). This procedure was aimed to extend the incubation time required for bacillary growth in the GC tube, thereby allowing sufficient time for the drug to act in the PZA-containing tube. By decelerating the growth rate in the GC, the system allows more time for PZA in the test tube to be converted to its active form, POA, and act against *M. tuberculosis*. This modification reduced the bacillary load in the PZA tube while preserving the acidified conditions required for PZA activity and minimizing the risk of false resistance due to alkalinization. Care was taken to ensure that the changes in inoculum volume did not significantly affect the initial pH (5.9) of the medium. After the addition of the OADC supplement (800 μL), the pH increased slightly. Further addition of 250 μL of culture suspension and sterile saline restored the pH back to acidic conditions, thereby maintaining the essential conditions for PZA activation. MGIT DST by the system is programmed in such a way that once the GC reaches GU of 400, the system finalizes the results according to the growth in the test sample. By lowering the bacillary burden in the GC tube, the time to the GU threshold was extended, thereby giving PZA more time to convert to POA, and act against viable bacilli in the PZA tube. If the GC reached GU 400 within ten days, suggesting insufficient bacillary elimination in the test tube, showing a GU >100, the result was interpreted as resistant. The rest of the procedure, including the reagent concentrations and incubation parameters, followed the standard MGIT PZA protocol. The SD MGIT DST method was also evaluated using a PZA concentration of 200 μg/mL for selected isolates.

2.5. Pyrazinamidase assay

PZase activity in the clinical isolates was assessed using Wayne's method (Sharma et al., 2010), Actively growing *M. tuberculosis* cultures, aged 3 weeks (21 days), were obtained from LJ slants. A heavy inoculum was obtained by scraping colonies from the LJ slant, which was directly stabbed into tubes containing the assay medium. The medium was prepared by combining Dubos broth base, 0.5 % agarose, 100 μg/mL pyrazinamide (PZA; Sigma-Aldrich), and 0.1 % sodium pyruvate. A volume of 5 mL of this mixture was dispensed into glass tubes and sterilized by autoclaving prior to inoculation. Agarose was substituted for agar to enhance the visibility of the colour. For each culture, duplicate PZase tubes were inoculated and incubated at 37 °C. Readings on the 4th and 7th days involved the addition of 1 ml of 1 % ferrous ammonium sulfate. The presence of any intensity of the pink band indicates the release of the PZase enzyme that determines the strain as susceptible. The absence of a pink band indicates a resistant strain with possible mutations in the *pncA* gene. *M. tuberculosis* strain H37Rv and *M. bovis* BCG were used as the positive and negative controls, respectively. Discordant or unclear results were repeated, and tubes showing contamination were excluded and retested.

2.6. DNA extraction and polymerase chain reaction (PCR)

DNA extraction was done by CTAB/NaCl (Hexadecyltrimethyl Ammonium Bromide/Sodium Chloride) method (Somerville et al., 2005). A loopful of bacterial culture was suspended in 100 μL of sterile distilled water and homogenized. The homogenate was treated with 50 μL lysozyme (10 mg/mL) and incubated overnight at 37 °C. Subsequently, 70 μL 10 % SDS and 6 μL Proteinase K (10 mg/mL) were added and incubated at 65 °C for 15 min. Next, 100 μL of 5 M NaCl and 80 μL of CTAB/NaCl were added and incubated at 65 °C for 10 min. To extract nucleic acids, 800 μL of chloroform:isoamyl alcohol (24:1) was added and centrifuged at 13,000 rpm for 10 min. The supernatant was transferred to a fresh tube, and DNA was precipitated by adding 600 μL isopropanol, followed by overnight incubation at −20 °C. DNA pellets were obtained by centrifugation at 12,000 rpm for 10 min at 4 °C, washed with 70 % ethanol, air-dried, and dissolved in 20 μL 1 × TE buffer.

Primers were specifically designed using Primer-BLAST to amplify the entire *pncA* gene, including its upstream promoter region, which encompasses positions −1 to −100 bp upstream of the *pncA* start codon (Miotto et al., 2014). The forward *pncA*F- GGCGTCATGGACCCTATATC, and reverse *pncA*R- CAACAGTTCATCCCGGTTC primers resulted in 670 bp of oligonucleotides used for amplification. PCR was performed under the following conditions: denaturation at 95 °C for 1 min, annealing at 56 °C for 30 s, and extension at 72 °C for 1 min. The amplified PCR product was purified using a QIAquick PCR Purification Kit. DNA concentration was determined using NanoDrop spectrophotometer.

2.7. Spoligotyping

Spoligotyping was performed using the standard methods (Driscoll, 2009). PCR was carried out on the isolated DNA with DR region amplification primers, Dra (GGTTTTGGGTCTGACGAC, 5′ biotinylated) and DRb (5′- CCGAGAGGGGACGGAAAC −3′), and the amplification products were hybridized to a Biodyne C membrane (Isogen Bioscience). Synthetic oligomeric spacer sequences immobilized on this membrane originate from the direct-repeat regions of *M. tuberculosis H37Rv* and *Mycobacterium bovis BCG*. Hybridized DNA was detected using an enhanced chemiluminescence kit. In comparison to the patterns existing in the SpolDB4 database, the acquired patterns were evaluated (Brudey et al., 2006; Demay et al., 2012).

2.8. Targeted DNA sequencing by Sanger method

DNA sequencing was performed on a Veriti® 96-Well Thermal Cycle (Applied Biosystems) using the Big Dye Terminator v3.1 Cycle Sequencing kit (Qiagen). A genetic sequencer 3500 genetic analyser (Applied Biosystems) was used for Sanger Sequencing. The same primer sets were used for sequencing PCR product. Each 10 μL reaction comprised the following components: 2 μL of the amplified PCR product (10 ng/μL), 1.75 μL of 5x Sequencing buffer, 0.5 μL of Big Dye Terminator solution, 2 μL of sequencing primers (1.6 pmoles/μL), and 3.75 μL of nuclease-free water. The reaction conditions were as follows: initial denaturation at 96 °C for 1 min (cycle 1), followed by polymerization at 96 °C for 10 s, 50 °C for 5 s, 60 °C for 4 min, and extension at 72 °C for 1 min. Followed this, 75 % isopropanol purification was performed and 10 μL of Hi-Di Formamide was added to the purified product before sequencing. The sequence data were compared with the reference strain

H37Rv and analyzed using Seq Scape software (version 3.0; Applied Biosystems, Foster City, CA) (Kumar et al., 2024).

2.9. Whole genome sequencing analysis

Paired-end whole-genome sequencing was performed using isolated DNAs. Sequence libraries were constructed using the Nextra XT DNA library preparation kit (Illumina) according to manufacturer's instructions and the resulting libraries were run on an Illumina HiSeq 2500 platform. Genome sequences were analyzed using MTBseq pipeline (https://github.com/ngs-fzb/MTBseq_source), which performs lineage classification based on phylogenetic single nucleotide polymorphisms and detects variant positions based on known associations with antibiotic resistance. Briefly, the filtered reads were aligned to the reference genome *M. tuberculosis* H37Rv (NC_000962), and variant calling was performed using the default parameters of the MTBseq pipeline, which included a minimum read coverage of 5 ×, a phred score ≥20, and an allele frequency threshold of 75 % for SNP confirmation. The sequences were further analyzed using the vSNP pipeline (https://github.com/USDA-VS/vSNP), which locates and validates SNPs and produces annotated SNP tables and their corresponding phylogenetic trees. The phylogenetic tree was further annotated to represent the lineage and observed resistance patterns using the Interactive Tree of Life (iTOL) (Letunic and Bork, 2021). The RD Analyzer (https://github.com/xiaeryu/RD-Analyzer) (Faksri et al., 2016) and RDScan were used to identify the regions of difference present within the sequences (https://github.com/dbespiatykh/RDscan) (Bespiatykh et al., 2021). ISMapper (version 2.0) (https://github.com/jhawkey/IS_mapper) was used to localize IS*6110* among the sequences with *M. tuberulosis* H37Rv (NC000962.3) as reference genome.

2.10. Drug resistance prediction

Genotypic resistance was predicted using TBProfiler (https://github.com/jodyphelan/TBProfiler) and GenTB (https://gentb.hms.harvard.edu) software. Both TBprofiler and GenTB recognize other variants in addition to previously reported resistance mutations. If the mutations identified in this study fall under the reported mutations or if it has been previously published in a peer-reviewed journal or reported in either the WHO mutation catalogue for *M. tuberculosis* (versions 1 and 2, 2021) (Shaojun and Xichao, 2024; WHO mutation catalogue, 2021) or in the Indian TB mutation catalogue (Indian mutation catalogue, 2022), they were classified as "previously reported". Those mutations that are exclusively found in this study for the first time and those that were not reported elsewhere and those that are not present in any of the mutation catalogues mentioned earlier were classified as "Novel". The mutations identified in this study were further compared with 100 resistant and sensitive South Indian isolates downloaded from the NCBI database to further confirm our findings.

3. Results

3.1. Lineage prediction by spoligotyping of the study isolates

Spoligotyping was done for the all the 401 study isolates and the lineage of the isolates were analyzed by using the spolDB4 database. The analysis revealed 176 (44 %) isolates as L1, 40 (10 %) isolates as L3, 25 (6.23 %) as L4, and 19 (4.73 %) isolates as L2. Strains exhibiting unique genetic patterns that did not align with any recognized lineage in the SITVITWEB database were classified as orphan strains, comprising 130 (32.4 %) of the total isolates (Demay et al., 2012). Furthermore, 11 isolates possessed a SIT number available in the SITVIT database; but, lacked a designated clade name (Table 1).

Table 1
Spoligotyping lineage distribution of 401 *M. tuberculosis* isolates analysed using spolDB4 databases.

SIT No	Octal No.	Clade	PZA pDST	No of isolates
6	077777777413731	L1-EAI1-SOM	Sensitive	3
8	400037777413771	L1-EAI5	Sensitive	6
11	477777777413071	L1-EAI3-IND	*Resistant*	12
11	477777777413071	L1-EAI3-IND	Sensitive	68
43	777777747413771	L1-EAI6-BGD1	Sensitive	2
48	777777777413731	L1-EAI1-SOM	*Resistant*	3
48	777777777413731	L1-EAI1-SOM	Sensitive	6
100	777777777773771	L1-EAI3-IND	Sensitive	3
120	477577777413071	L1-EAI3-IND	Sensitive	3
126	477777777413771	L1-EAI5	*Resistant*	1
126	477777777413771	L1-EAI5	Sensitive	15
138	777777777413700	L1-EAI5	Sensitive	1
236	777777777413771	L1-EAI5	Sensitive	4
256	777777777413671	L1-EAI5	Sensitive	1
298	477767777413071	L1-EAI3-IND	Sensitive	1
338	077777777413071	L1-EAI3-IND	Sensitive	4
340	474377777413771	L1-EAI5	Sensitive	13
342	677777777413771	L1-EAI5	Sensitive	3
355	477777777413031	L1-EAI3-IND	Sensitive	11
414	477777767413071	L1-EAI3-IND	Sensitive	1
473	401777777413071	L1-EAI3-IND	Sensitive	2
475	477776077411771	L1-EAI5	*Resistant*	1
591	777777757413771	L1-EAI6-BGD1	Sensitive	5
763	777700777413700	L1-EAI5	Sensitive	1
1182	477777777413731	L1-EAI1-SOM	Sensitive	3
1956	467777777413071	L1-EAI3-IND	Sensitive	5
1966	477777777413011	L1-EAI5	Sensitive	1
1983	474000377413031	L1-EAI3-IND	Sensitive	1
2452	477774377413071	L1-EAI3-IND	Sensitive	4
2465	477777757413771	L1-EAI3-IND	Sensitive	1
2698	777777743763771	L1-MANU2	Sensitive	1
1	000000000003771	L2-Beijing	Sensitive	17
616	400000000003771	L2-Beijing	Sensitive	1
1187	000002000003771	L2-Beijing	*Resistant*	1
25	703777740003171	L3-CAS1-Delhi	Sensitive	2
26	703777740003771	L3-CAS1-Delhi	*Resistant*	2
26	703777740003771	L3-CAS1-Delhi	Sensitive	13
142	703777700003771	L3-CAS1-Delhi	Sensitive	1
288	700377740003771	L3-CAS2	Sensitive	7
289	703777740003571	L3-CAS1-Delhi	Sensitive	1
1264	703777740000000	L3-CAS1-Delhi	Sensitive	1
1320	700177740003771	L3-CAS2	Sensitive	4
2100	700377700003771	L3-CAS	Sensitive	3
40	777777377760771	L4-T4	Sensitive	1
42	777777607760771	L4-LAM9	*Resistant*	1
47	777777774020771	L4-H1	Sensitive	2
50	777777777720771	L4-H3	Sensitive	2
52	777777777760731	L4-T2	Sensitive	1
53	777777777760771	L4-T1	*Resistant*	2
53	777777777760771	L4-T1	Sensitive	4
119	777776777760771	L4-X1	Sensitive	2
163	777777607760700	L4-LAM4	Sensitive	1
200	700076777760700	L4-X3	Sensitive	1
281	777775777760771	L4-T1	*Resistant*	2
281	777775777760771	L4-T1	Sensitive	1
397	777777600000771	L4-LAM	Sensitive	1
512	777777707720771	L4-H3	Sensitive	1
787	777777777760071	L4-T1	Sensitive	1
1324	777760047760771	L4-T2	Sensitive	1
1367	377737607760771	L4-LAM5	Sensitive	2
124	777777777700771	Unknown	Sensitive	6
1275	777777774000371	Unknown	Sensitive	1
1952	777777774000771	Unknown	Sensitive	3
2704	677777457413771	Unknown	Sensitive	1
	777777740363771	Orphan strain	Sensitive	1
	777777000360731	Orphan strain	Sensitive	1
	777777774005771	Orphan strain	Sensitive	1
	500033000001771	Orphan strain	Sensitive	1
	500573000003771	Orphan strain	Sensitive	1
	473776077411771	Orphan strain	Sensitive	1
	474377777413731	Orphan strain	Sensitive	1
	477777777413571	Orphan strain	Sensitive	2
	763777747413771	Orphan strain	Sensitive	1

(*continued on next page*)

Table 1 (*continued*)

SIT No	Octal No.	Clade	PZA pDST	No of isolates
	677777777413071	Orphan strain	Sensitive	3
	567777777413571	Orphan strain	Sensitive	1
	677777476001771	Orphan strain	Sensitive	1
	674377777413771	Orphan strain	Sensitive	1
	677775777413071	Orphan strain	Sensitive	1
	477400177413071	Orphan strain	Sensitive	4
	474017777413071	Orphan strain	Sensitive	1
	776177753011571	Orphan strain	Sensitive	1
	476777777013571	Orphan strain	Sensitive	1
	476777777013071	Orphan strain	Sensitive	1
	476777770013771	Orphan strain	Sensitive	1
	400000177413571	Orphan strain	Sensitive	1
	403777777413071	Orphan strain	Sensitive	2
	701777740003671	Orphan strain	Sensitive	1
	477774302413071	Orphan strain	Sensitive	1
	677777777413571	Orphan strain	Sensitive	5
	460000077003071	Orphan strain	Sensitive	1
	500033000000771	Orphan strain	Sensitive	1
	545533000003771	Orphan strain	Sensitive	1
	777777377761771	Orphan strain	Sensitive	1
	677673177413571	Orphan strain	Sensitive	1
	200272100003771	Orphan strain	Sensitive	1
	677777777412000	Orphan strain	Sensitive	1
	400000377413071	Orphan strain	Sensitive	6
	000012000003771	Orphan strain	Sensitive	1
	773777700003071	Orphan strain	Sensitive	1
	474377777413571	Orphan strain	Sensitive	1
	577777777407171	Orphan strain	Sensitive	6
	477777777413001	Orphan strain	Sensitive	2
	477777703413071	Orphan strain	Sensitive	1
	777777737760621	Orphan strain	Sensitive	1
	733377740003771	Orphan strain	Sensitive	1
	440377777413171	Orphan strain	Sensitive	1
	477777777413051	Orphan strain	Sensitive	1
	401777777413031	Orphan strain	Sensitive	3
	703767700000061	Orphan strain	Sensitive	1
	377777477413771	Orphan strain	Sensitive	1
	400037777413711	Orphan strain	Sensitive	1
	377777777413771	Orphan strain	Sensitive	2
	077774400000200	Orphan strain	Sensitive	1
	477777766000071	Orphan strain	Sensitive	1
	400777777413031	Orphan strain	Sensitive	1
	501777740003661	Orphan strain	Sensitive	1
	777777777737771	Orphan strain	Sensitive	1
	774377777437771	Orphan strain	Sensitive	1
	640372363777711	Orphan strain	*Resistant*	1
	577777770000771	Orphan strain	Sensitive	1
	474377377413771	Orphan strain	Sensitive	1
	474000377413071	Orphan strain	Sensitive	1
	700370740003771	Orphan strain	Sensitive	1
	777737543560771	Orphan strain	Sensitive	1
	777737757413371	Orphan strain	Sensitive	1
	700175177760671	Orphan strain	Sensitive	1
	467377777413031	Orphan strain	Sensitive	1
	777777407700071	Orphan strain	Sensitive	1
	777777660020771	Orphan strain	Sensitive	1
	400057777413771	Orphan strain	Sensitive	1
	077767777413621	Orphan strain	Sensitive	1
	513767740003661	Orphan strain	Sensitive	1
	474377777413671	Orphan strain	Sensitive	2
	474777777407771	Orphan strain	Sensitive	1
	077777017413731	Orphan strain	Sensitive	1
	477774202001071	Orphan strain	Sensitive	1
	477777777417771	Orphan strain	Sensitive	1
	477777777413471	Orphan strain	Sensitive	1
	777777777777371	Orphan strain	Sensitive	1
	477777777417071	Orphan strain	Sensitive	2
	777737757411371	Orphan strain	Sensitive	1
	476077777410071	Orphan strain	Sensitive	1
	477774200013071	Orphan strain	Sensitive	1
	477777770013071	Orphan strain	Sensitive	1
	500066677760600	Orphan strain	Sensitive	1
	463777777413071	Orphan strain	Sensitive	1
	700037777413771	Orphan strain	Sensitive	1
	701777700003771	Orphan strain	Sensitive	1
	777757777600561	Orphan strain	Sensitive	1

Table 1 (*continued*)

SIT No	Octal No.	Clade	PZA pDST	No of isolates
	476000003413071	Orphan strain	Sensitive	1
	401777777017071	Orphan strain	Sensitive	1
	707777777700771	Orphan strain	Sensitive	1
	477037777413771	Orphan strain	Sensitive	1
	501047600003661	Orphan strain	Sensitive	1
	777774007413771	Orphan strain	Sensitive	1
	700777700017771	Orphan strain	Sensitive	1
	777777777764621	Orphan strain	Sensitive	1
	473777037411771	Orphan strain	*Resistant*	1
	777777777412031	Orphan strain	*Resistant*	1
	667777777413031	Orphan strain	*Resistant*	1
	473776077411771	Orphan strain	*Resistant*	1
	400000007777711	Orphan strain	*Resistant*	1

3.2. Phenotypic DST outcomes of standard and RI MGIT DST and Waynes's assay

Standard MGIT DST was performed initially on a subset of 100 /401 *M. tuberculosis* isolates among which 73/100 (73 %) isolates were identified as sensitive and 27/100 isolates (27 %) as resistant. Whereas, Wayne's assay performed in parallel for these 100 isolates, identified all 100 isolates as sensitive. The results observed by both these methods were highly incongruent, hence DST was performed using the RI MGIT DST method (Piersimoni et al., 2013), which identified only 2/100 (2 %) isolates as resistant. Owing to the considerable reduction in false-resistant results, the remaining samples (301/401) were tested only with the RI MGIT DST method, which identified 47/401 (11.7 %) as resistant and 354/401 (88.3 %) as sensitive. However, only 13/401 (3.2 %) were found to be resistant by Wayne's method. A comparative analysis of the two methods demonstrated that Wayne's assay had a sensitivity of 41.9 %, specificity of 100 %, and F1 score of 0.59. However, 34/47 isolates (72.34 %) classified as susceptible by Wayne's assay were determined to be resistant by RI MGIT DST, reflecting the need for comprehensive testing to avoid false resistance classifications. The high specificity of Wayne's assay ensures that it can accurately rule out false resistance, but its moderate sensitivity necessitates the use of RI MGIT DST for reliable identification of resistant isolates. The difference in resistant strains observed in both these methods might owe to the nature of the phenotypic assays, wherein the RI MGIT DST method directly assesses phenotypic resistance, whereas the Wayne's method focuses only on PZase production, providing a complementary yet distinct perspective. So, the isolates classified as resistant only by the RI MGIT DST assay, suggest the existence of alternative resistance mechanisms beyond *pncA* mutations or PZase activity disruption.

3.3. Comparison of SD MGIT DST and assessment of PZA concentration

To address the discrepancy between the RI MGIT DST (11.7 %) and Wayne's assay (3.2 %), and to potentially reduce false resistance detected, RI MGIT DST was further modified. This modified SD MGIT DST was applied to a total of 100 isolates consisting of all the 47 isolates previously identified as resistant and an additional 53 randomly selected phenotypically sensitive isolates. The sample inoculum was further diluted to 1:50 instead of the 1:20 used in the RI MGIT DST method. This dilution precisely controls the bacterial load and drug exposure conditions providing ample time for the growth unit in the GC to reach 400. This method identified only 31/47 isolates as resistant and 16/47 isolates as sensitive. However, all the 53 sensitive isolates were confirmed as sensitive. This result suggests that the modified SD MGIT DST method reduced the false-resistance rate from 11.7 to 7.7 % while maintaining specificity and improving the concordance with Wayne's assay. This modified method was not applied to the entire set of 401 samples. The reduced rate likely reflects a more accurate determination of resistance, reinforcing the critical role of optimized DST conditions for reliable phenotypic results.

To further validate the SD MGIT DST method and evaluate the resistance stability, all 47 isolates identified as resistant by RI MGIT DST were tested with 200 μg/mL PZA. The results showed that only 25/47 maintained resistance at 200 μg/mL PZA with > 100 GU, and the remaining 22/47 isolates had < 100 GU classifying as sensitive (Table 2). These findings support the improved performance of the SD MGIT DST method and also indicate that 100 μg/mL acts as a crucial cut-off point for detecting PZA resistance, encompassing a wider spectrum of resistant phenotypes. However, the stronger correlation with resistance observed at 200 μg/mL suggests its effectiveness as a more stringent indicator of high-level resistance, consistent with previously established MIC-based classes of resistance severity (Stoffels et al., 2012).

3.4. Genotypic findings: pncA mutations

Targeted sequencing of the *pncA* gene was performed for all 401 isolates, among which only 14 isolates revealed mutations in the *pncA* gene, which is among the 31 isolates classified as resistant by the SD MGIT DST. Among these, 9 isolates carried mutations in the genes listed in the WHO mutation catalogue, confirming their established role in PZA resistance and validating our findings (WHO mutation catalogue, 2021). Two isolates harbored mutations reported in the literature (Miotto et al., 2014) and one isolate in the Indian mutation catalogue (Indian mutation catalogue, 2022), reflecting the diversity of mutations linked to resistance. One isolate with a Cys14Phe mutation in *pncA* was identified as susceptible by Wayne's method and reported as neutral elsewhere (Maharaj, 2016). Notably, one isolate (Sample no. KP126) contained *pncA* (Del_2289115–2289127gatggtag) mutation that have not been previously reported, suggesting novel mutations leading to PZA resistance (Table 3). The absence of *pncA* mutations in the remaining resistant isolates suggests alternative resistance mechanisms beyond *pncA*. This signifies the complexity of PZA resistance and potential involvement of other genomic factors. Additionally, synonymous mutations in *pncA* gene were observed in 19/388 isolates identified as sensitive by Wayne's method, indicating possible natural polymorphisms that may not have a direct impact on PZA resistance.

Table 2
Comparative assessment of phenotypic methods among the resistant isolates identified in this study.

S.no	Sample ID	ICT-MPT64	INH	RIF	RI MGIT DST 100 μg/ml	SD MGIT DST		Wayne's/PZase Assay
						100 μg/ml	**200 μg/ml**	
1	KP126	POS	R	R	R (GU_400)	R (GU_400)	R (GU_400)	R
2	KP128	POS	R	R	R (GU_400)	R (GU_400)	R (GU_400)	S
3	KP159	POS	R	R	R (GU_400)	R (GU_400)	R (GU_400)	R
4	KP163	POS	R	S	R (GU_400)	R (GU_400)	R (GU_400)	R
5	KP184	POS	R	R	R (GU_400)	R (GU_400)	R (GU_400)	R
6	KP194	POS	R	S	R (GU_400)	R (GU_400)	R (GU_400)	R
7	KP207	POS	R	R	R (GU_400)	R (GU_400)	R (GU_400)	R
8	KP226	POS	R	R	R (GU_400)	R (GU_400)	R (GU_400)	R
9	KP228	POS	R	R	R (GU_400)	R (GU_400)	R (GU_240)	R
10	KP234	POS	R	R	R (GU_400)	R (GU_400)	R (GU_400)	R
11	KP236	POS	R	R	R (GU_400)	R (GU_400)	R (GU_400)	R
12	KP282	POS	R	S	R (GU_400)	R (GU_400)	S (GU_93)	R
13	KP363	POS	R	S	R (GU_400)	R (GU_400)	R (GU_400)	R
14	KP377	POS	R	S	R (GU_400)	R (GU_400)	S (GU_76)	R
15	KP012	POS	S	S	R (GU_400)	R (GU_400)	R (GU_400)	S
16	KP102	POS	R	S	R (GU_400)	R (GU_400)	R (GU_400)	S
17	KP123	POS	R	R	R (GU_400)	R (GU_400)	R (GU_377)	S
18	KP138	POS	R	S	R (GU_400)	R (GU_400)	S (GU_48)	S
19	KP162	POS	R	S	R (GU_400)	R (GU_400)	R (GU_400)	S
20	KP196	POS	R	S	R (GU_400)	R (GU_400)	R (GU_400)	S
21	KP222	POS	R	R	R (GU_400)	R (GU_400)	R (GU_400)	S
22	KP242*	POS	S	S	R (GU_356)	R (GU_400)	R (GU_400)	S
23	KP245*	POS	S	S	R (GU_400)	R (GU_400)	R (GU_400)	S
24	KP252*	POS	S	S	R (GU_400)	R (GU_400)	S (GU_0)	S
25	KP279*	POS	S	S	R (GU_400)	R (GU_400)	R (GU_400)	S
26	KP367	POS	S	S	R (GU_400)	R (GU_257)	S (GU_0)	S
27	KP383*	POS	S	S	R (GU_400)	R (GU_400)	R (GU_400)	S
28	KP392*	POS	S	S	R (GU_400)	R (GU_400)	R (GU_400)	S
29	KP403*	POS	S	S	R (GU_400)	R (GU_400)	R (GU_400)	S
30	KP440*	POS	S	S	R (GU_400)	R (GU_400)	R (GU_400)	S
31	KP455*	POS	S	S	R (GU_400)	R (GU_400)	S (GU_68)	S
32	KP49	POS	S	S	R (GU_400)	S (GU_0)	S (GU_0)	S
33	KP145	POS	R	S	R (GU_400)	S (GU_0)	S (GU_0)	S
34	KP153	POS	R	R	R (GU_400)	S (GU_77)	S (GU_0)	S
35	KP154	POS	R	S	R (GU_400)	S (GU_0)	S (GU_0)	S
36	KP161	POS	R	R	R (GU_295)	S (GU_0)	S (GU_0)	S
37	KP166	POS	R	R	R (GU_400)	S (GU_0)	S (GU_0)	S
38	KP195	POS	R	S	R (GU_400)	S (GU_0)	S (GU_0)	S
39	KP233	POS	S	S	R (GU_400)	S (GU_0)	S (GU_0)	S
40	KP277	POS	S	S	R (GU_400)	S (GU_0)	S (GU_0)	S
41	KP341	POS	S	S	R (GU_400)	S (GU_0)	S (GU_0)	S
42	KP361	POS	S	S	R (GU_400)	S (GU_76)	S (GU_0)	S
43	KP366	POS	S	S	R (GU_400)	S (GU_0)	S (GU_0)	S
44	KP383	POS	S	S	R (GU_400)	S (GU_0)	S (GU_0)	S
45	KP408	POS	R	S	R (GU_400)	S (GU_18)	S (GU_0)	S
46	KP435	POS	S	S	R (GU_400)	S (GU_0)	S (GU_0)	S
47	KP458	POS	S	S	R (GU_400)	S (GU_0)	S (GU_0)	S

Abbreviations: ICT - MPT64: Immuno chromatographic test for MPT64 antigen for *M. tuberculosis* complex. Pos - Positive; INH - Isoniazid; RIF - Rifampicin; RI MGIT DST - Reduced inoculum method; SD MGIT DST - Sparse dilution method; R - Resistant; S - Sensitive; GU - Growth unit; *- PZA mono resistant identified by TB profiler WGS results.

Table 3
Details of phenotypic and genotypic assays and mutations observed in all the resistant isolates identified in this study.

S. no	Sample ID	SD MGIT DST	Targeted *pncA* sequencing		*WGS results*			*Lineage prediction*		Reference
		100 µg/ml	**NT**	**AA**	**Gene**	**Mutation**	**Type of mutation**	**WGS**	**Spoligotyping**	
1	KP126	R	Del at 118–127	Frameshift	*pncA*	Del_2,289,115–2289127gatggtag	Frameshift	L1-EAI1	EAI1-SOM	Unreported
2	KP128	R	G41T	Cys14Phe	*pncA*	p.Cys14Phe	Non-synonymous	L1-EAI3	EAI3-IND	(Maharaj, 2016)
3	KP159	R	G289T	Gly97Cys	*pncA*	p.Gly97Cys	Non-synonymous	L1-EAI3	EAI3-IND	(WHO mutation catalogue, 2021)
4	KP163	R	G ins at 392	Frameshift at codon 131	*pncA*	INS_i391G_131G	Frameshift	L4-H37Rv like	T1	(Khan et al., 2019; Miotto et al., 2014)
5	KP184	R	C24G	Asp8Glu	*pncA*	p.Asp8Glu	Non-synonymous	L4-T	T1	(WHO mutation catalogue, 2021)
6	KP194	R	T254G	Leu85Arg	*pncA*	p.Leu85Arg	Non-synonymous	L1-EAI3	EAI3-IND	(WHO mutation catalogue, 2021)
						Del_CF_2,288,718_D524atctcctcca_2,288,727	Frameshift			Unreported
7	KP207	R	G533T	Val180Phe	*pncA*	p.Val180Phe	Non-synonymous	L4-LAM	LAM9	(WHO mutation catalogue, 2021)
8	KP226	R	A152C	His51Pro	*pncA*	p.His51Pro	Non-synonymous	L1-EAI3	EAI3-IND	(WHO mutation catalogue, 2021)
9	KP228	R	G538T	Val180Phe	*pncA*	p.Val180Phe; Rv0191c_Met381Thr	Non-synonymous	L1-EAI3	EAI3-IND	(WHO mutation catalogue, 2021)
10	KP234	R	T515C	Leu172Pro	*pncA*	p.Leu172Pro	Non-synonymous	L2-Non-Beijing	Orphan strain	(WHO mutation catalogue, 2021)
11	KP236	R	T559G	Stop codon at 187Gly	*pncA*	p.187Gly	Non-synonymous	L2-Beijing	Beijing	(Indian mutation catalogue, 2022)
12	KP282	R	T515C	Leu172Pro	*pncA*	p.Leu172Pro	Non-synonymous	L2-Non-Beijing	Orphan strain	(WHO mutation catalogue, 2021)
13	KP363	R	G ins at 392	Frameshift at codon 131	*pncA*	*pncA* c.391dupG	Frameshift	L4-H37Rv-like	T1	(Miotto et al., 2014)
14	KP377	R	A146C	Asp49Ala	*pncA*	p.Asp49Ala	Non-synonymous	L3-Delhi-CAS	CAS1-Delhi	(WHO mutation catalogue, 2021)
						Upstream gene_c.−125delC	Frameshif			Unreported
15	KP012	R	Nil	Nil	*glpK*	Del_GAP_4,138,373	Frameshift	L3-CAS	CAS1-Delhi	Unreported
16	KP102	R	Nil	Nil	*panD* *Rv1258c*	p.Ile49Val p.val280Leu	Non-synonymous	L1-EAI1	Orphan strain	(Werngren et al., 2017)
17	KP123	R	Nil	Nil	NA	NA	NA	L1-EAI1	EAI3-IND	–
18	KP138	R	Nil	Nil	NA	NA	NA	L1-EAI1	EAI3-IND	–
19	KP162	R	Nil	Nil	*panD* *Rv1258c*	p.Ile49Val p.val280Leu	Non-synonymous	L1-EAI3	EAI5	(Werngren et al., 2017)
20	KP196	R	Nil	Nil	*Mas*	p.Val1034Met	Non-synonymous	L4-X type	T1	Unreported
21	KP222	R	Nil	Nil	*Rv3008c*	p.Leu32Pro	Non-synonymous	L1-EAI3	EAI3-IND	Unreported
22	KP242	R	Nil	Nil	*Mas*	p.Ile1808Thr	Non-synonymous	L1-EAI3	EAI3-IND	Unreported
23	KP245	R	Nil	Nil	*lprG*	p.Arg157Gln	Non-synonymous	L1-EAI1	Orphan strain	Unreported
24	KP252	R	Nil	Nil	NA	NA	NA	L1-EAI3	EAI3-IND	–

(*continued on next page*)

Table 3 (*continued*)

S. no	Sample ID	SD MGIT DST	Targeted *pncA* sequencing		*WGS results*			*Lineage prediction*		Reference
		100 µg/ml	**NT**	**AA**	**Gene**	**Mutation**	**Type of mutation**	**WGS**	**Spoligotyping**	
25	KP279	R	Nil	Nil	*Mas*	p.Asp286Glu	Non-synonymous	L1-EAI1	EAI1-SOM	Unreported
26	KP367	R	Nil	Nil	*Rv0191*	p.Ala303Thr	Non-synonymous	L1-EAI1	EAI1-SOM	Unreported
27	KP383	R	Nil	Nil	*Mas*	p.Ala1911Gly	Non-synonymous	L1-EAI3	EAI3-IND	Unreported
28	KP392	R	Nil	Nil	NA	NA	NA	L1-EAI3	Orphan strain	–
29	KP403	R	Nil	Nil	*panD* *Rv1258c*	p.Ile49Val p.Val280Leu	Non-synonymous	L1-EAI	Orphan strain	(Werngren et al., 2017)
30	KP440	R	Nil	Nil	*Rv1258c*	p.Val280Leu	Non-synonymous	L1-EAI3	EAI5	Unreported
31	KP455	R	Nil	Nil	*Rv3008c*	p.Leu32Pro	Non-synonymous	L1-EAI3	EAI3-IND	Unreported

Abbreviations: SD MGIT DST - Sparse dilution method; NC - Nucleotide change; AA - Amino acid change; NIL – No mutation in *pncA*; R - Resistant.
- Novel mutations; *pncA* - Pyrazinamidase; *panD* - Aspartate decarboxylase; *glpK* - Glycerol kinese; *mas* - Mycocerosic acid synthase *and lprG* - Lipoprotein. NA- No mutations observed in the target genes linked to PZA resistance.

3.5. Genotypic findings: alternative PZA resistance genes

Whole genome sequencing was performed on all 31/401 isolates identified as resistant, along with 11 isolates that were phenotypically sensitive, using the SD MGIT DST method to analyze the genes and mutations associated with resistance. For each isolate, WGS yielded an average of 6 million reads (range, 2 – 14 million), with an average read length of 151 base pairs and an average coverage depth of 227 (range, 65 – 387). Additional associated features were detailed in **Supplementary table S2**. WGS identified *pncA* mutations in 14 isolates, which was concordant with the results of targeted sequencing. Of these, two isolates exhibited two different *pncA* variants, of which p.Leu85Arg and p.Asp49Ala have been previously reported. The other mutations in the upstream region of Rv2044c_c.−125delC and Del_CF_2288718_D524atctcctcca_2288727 in the *pncA* gene identified by WGS have not been previously reported, suggesting novel mutations leading to PZA resistance (Table 3). In alternative mechanisms, 3 isolates had mutations in *panD* gene, which has already been reported for PZA resistance. Additionally, 4 isolates had mutations in the *mas* gene, 1 isolate in the *glpk* gene and 1 in *lprG* gene. To the best of our knowledge, this is the first study to observe mutations in these genes among clinical isolates instead of *in vitro* mutant strains induced by POA. Mutations in the PZA resistance associated efflux pump genes (*Rv3008c, Rv0191c*, and *Rv1258c*) were observed in 4 of isolates; however, the position of the mutations and amino acid changes observed in these genes were novel. Nevertheless, 4 isolates did not possess any mutations in any of the target genes contributing to PZA resistance, as reported in the WHO mutation catalogue. In addition, ISMapper analysis determined that there were no IS*6110* insertions in the *pncA* and other genes of PZA resistant isolates. The observed mutations in the resistant isolates were absent in sensitive isolates. These findings underscore the genetic diversity underlying PZA resistance, and all the novel mutations identified in this study are tabulated (Table 4). Furthermore, PZA resistance was mostly observed in MDR-TB cases (12/31; 38.7 %), PZA with INH resistance in 8/31 (25.8 %), PZA mono-resistance in 9/31 (29 %), and PZA with other TB drugs in 2/31, according to TB profiler drug prediction analysis (Phelan et al., 2019). A phylogeny was generated, with all 31 resistant isolates showing the lineage and mutations observed (Fig. 2). The predominant lineage among the resistant population was *M. tuberculosis* Lineage-4, identified in 5/25 (20 %) isolates, followed by Lineage-2 in 3/19 (15.7 %), Lineage-1 in 21/176 (11.9 %), and Lineage-3 in 2/40 (5 %) isolates.

Table 4
Novel mutations identified in *M. tuberculosis* isolates ($n = 31$) resistant to PZA.

Gene Name	No. of Isolates	Mutations	Genome Position
pncA	1	Del_115–127gatggtag (Frameshift)	2289,115 – 2289,127
pncA	1	Del_CF_D524atctcctcca_175 (Frameshift)	2288,718 - 2288,727
pncA	1	Upstream gene_c.−125delC	2289,365
glpK	1	Del_GAP (Frameshift)	4138,373
lprG	1	G470A (R157Q)	1588,013
Mas	1	G3100A (V1034M)	3279,616
Mas	1	C858G (D286E)	3281,858
Mas	1	C5732G (A1911G)	3276,984
Rv3008c	2	T95C (L32P)	3366,738
Rv0191c	1	G907A (A303T)	223,195
Rv1258c	1	G838C (V280L)	1406,503

Abbreviations: Del- deletion; *pncA* - Pyrazinamidase; *mas*- Mycocerosic acid synthase; *glpK*- glycerol kinase and, *lprG*- Lipoprotein-triacylglyceride.

3.6. Evaluation of genotypic mutations with phenotypic resistance

WGS revealed additional mutations in other PZA resistant associated genes like *glpK, mas*, and *lprG* in clinical isolates that were phenotypically resistant to PZA, some of which had not been previously reported. To determine the novelty and potential association of these mutations with resistance, a comparative analysis using publicly available whole genome sequences was performed. Phenotypically PZA sensitive and PZA resistant isolates from South India from the project PRJNA822663 (Shanmugam et al., 2022) was downloaded for this purpose. Mutations identified in the resistant isolates were checked against these external datasets. Variants that were absent in both sensitive and resistant isolates from the same region were flagged as novel and the variants that were absent in all sensitive isolates but present in other resistant isolates were considered potentially resistance-associated. If such variants had not been previously reported in the literature or databases, they were also classified as novel. Detailed information on the downloaded sequences, the lineages and susceptibility profiles, and mutations identified in *pncA* and other genes associated with PZA resistance are provided in **Supplementary table S1**.

We analyzed 142 sequences, inclusive of 100 sequences comprising of 69 resistant and 31 sensitive isolates downloaded from NCBI, along with 31 resistant and 11 sensitive isolates from this study. Among these, 100/142 were resistant, and 42/142 were phenotypically sensitive. Among the 100 phenotypically resistant isolates, 52/100 had mutations in the *pncA* gene and 23/100 in alternate genes. Whereas 5/100 had

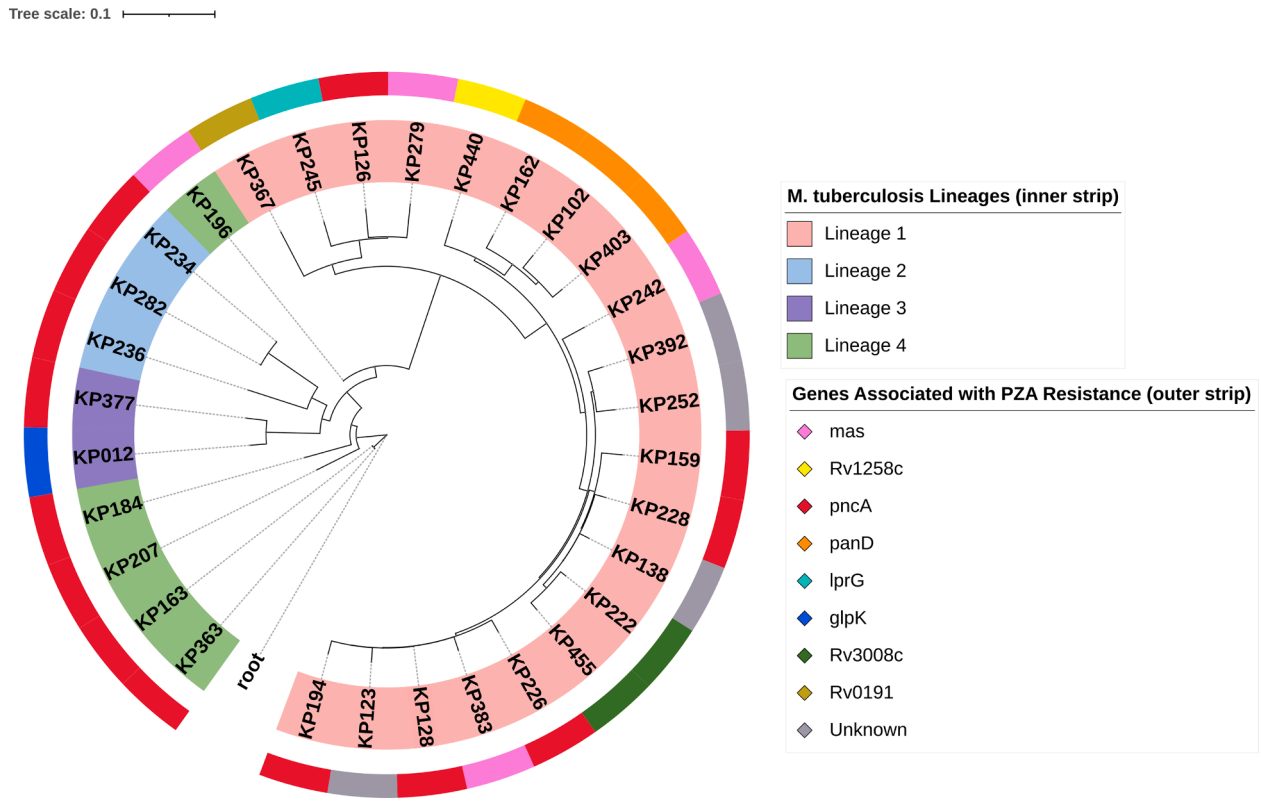

Fig. 2. Phylogenetic tree representing all the 31 resistant isolates identified in this study. The colored ranges represent the lineage distribution among the isolates and the outer strip indicates the target genes linked to PZA resistance.

mutations in both *pncA* and alternative genes and the remaining 20/100 isolates harbored no mutations in the target genes related to PZA resistance. Additionally, mutations in the *pncA* gene (Val180Phe and Thr142Lys) and *rpsA* (Ile139Ser) were found in 2 and 1 of the sensitive isolates, respectively.

In regard with the alternative mechanism, mutations in *mas* gene 8/23, *panD* 4/23, *Rv0191* 3/23, *rpsA* 1/23, *lprG* 2/23, *Rv1258* 2/23, Rv3008 2/23, and *glpK* 1/23 observed in the resistant isolates were absent in PZA-sensitive isolates. Whereas mutations in *clpC1* (val63Ala), *glpK* (val460Ala; A ins C_4139183), *mas* (Ala294Glu; Arg862Trp; Ala810Thr; Gly1842Glu; His1498Try; Thr2005Pro), Rv0191 (Ala213Thr), *Rv1258c* (T ins G_1406760), Rv3236c (Thr102Ala) and PPE35 (Leu896Ser, Gly877Asp, Gly624Asp, Gly415Ala) were observed in both sensitive and resistant isolates.

Our findings revealed that mutations in *lprG* (Arg157Gln), *mas* (Val1034Met; Ile1808Thr; Asp286Glu; and Ala1911Gly), and *glpK* (Del_GAP at 4138373), and efflux mechanisms *Rv0191* (Ala303Thr), *Rv1258* (Val280Leu), and *Rv3008* (Leu32Pro) were absent in all PZA-sensitive isolates used for analysis. However, the mutation Ile1808Thr in the *mas* gene, identified only in the resistant isolates in our study, was recently reported in sensitive PZA strain (Tamilzhalagan et al., 2025). The mutations in *lprG, mas, Rv0191, and Rv1258* genes identified in our resistant isolates were also observed in the other resistant strains included in our analysis, although these mutations have not been previously reported. Whereas the mutations in *glpk* and Rv3008 were present only in our study isolates (Table 5).

Table 5
Alternative mechanisms identified in this study were verified among retrieved sequence data.

Alternative mechanisms	Mutation	Number of study isolates	Downloaded isolates from NCBI	Resistance phenotype in retrieved data	Gene function
panD	Ile49Val	3	1	R	Aspartate decarboxylase PanD, involved in Coenzyme A biosynthesis (Sun et al., 2020)
lprG	Arg157Gln	1	0	R	Conserved lipoprotein, binds triacylated glycolipids leading to drug tolerance (Martinot et al., 2016a)
	His59Gln	0	1		
mas	Val1034Met	1	0	R	Multifunctional mycocerosic acid synthase membrane, involved in phthiocerol dimycocerosate (PDIM) synthesis (Gopal et al., 2016)
	Ile1808Thr	1	4		
	Asp286Glu	1	0		
	Ala1911Gly	1	0		
	Ile2083Leu	0	1		
glpk	Del_GAP_4,138,373	1	0	R	Glycerol kinase, involved in glycerol catabolism (Safi et al., 2019)
Rv0191	Ala303Thr	1	1	R	Conserved integral membrane protein, involved in transport of drug across the membrane (Zhang et al., 2017)
	Val250Ile	0	1		
Rv1258	Val280Leu	4	2	R	Putative multidrug efflux pump, encodes a tetracycline/ aminoglycoside resistance (TAP-2)-like efflux pump (J. Liu et al., 2019; Sharma et al., 2010)
	Gly416Val	0	1		
Rv3008	Leu32Pro	2	0	R	Uncharacterized membrane protein YhiD, involved in acid resistance (Zhang et al., 2017)

4. Discussion

The emergence of drug-resistant TB poses a significant and formidable global public health threat, particularly in regions with limited resources (Lv et al., 2024). The current study employed two phenotypic methods to investigate PZA resistance in presumptive drug-resistant TB, and subsequently correlated these findings with genotypic approaches. The BD BACTEC MGIT 960 PZA kit, widely used under India's National Tuberculosis Elimination Programme (NTEP) for phenotypic PZA susceptibility testing, utilizes an acidified medium optimized for PZA activity (PMDT guidelines, 2021).

The finding of the PZA resistance was initially 27 %, which did not align with Wayne's assay and targeted *pncA* sequencing results. The observed false resistance in phenotypic DST may be attributed to a high inoculum of *M. tuberculosis*, which can raise the pH of the culture medium, diminishing PZA activity (Mustazzolu et al., 2017). Upon employing the RI MGIT DST method, PZA resistance dropped to 11.7 %, although these findings still were not congruent with either the Wayne's assay nor the targeted sequencing.

To overcome this, we employed SD MGIT DST method, which further reduced the inoculum to 1:50 compared to 1:20 by RI MGIT DST method. This modification decreases the bacilli load in the GC tube, allowing ample time for the drug to act in the PZA test tube. As a result, PZA resistance decreased from 11.7 % to 7.7 %, with a 4.1 % reduction in false -resistant rates. These results aligned more closely with the genotypic findings, providing credence for the SD MGIT DST approach. Previous reports from Southern India reported 43 % phenotypic PZA resistance, among which only 36.5 % had a genotypic correlation (Indian mutation catalogue, 2022). Shanmugam et al. (2022) found that among the 66 % (119/181) of phenotypic PZA resistance, 62 isolates did not have any known mutations (Shanmugam et al., 2022). These findings highlight the importance of using the SD MGIT DST method to improve the accuracy.

Our approach differs from Morlock et al. (2017), who employed different dilution strategies for both the control and PZA tubes. In contrast, the SD MGIT DST method focused on reducing the dilution in the GC tube to 1:50, and the inoculum volume was reduced to 250 μL and compensated with 250 μL of sterile saline in both control and PZA tubes. This effectively reduced the bacterial load, while maintaining the overall test volume and pH. This step was performed to minimize false resistance, while simplifying the procedure compared to the dual-dilution methods. Given that acidic pH slows *M. tuberculosis* metabolism and growth, this method prevents rapid overgrowth in the GC tube and ensures prolonged exposure of bacilli to PZA. Extending the incubation period further accommodated the slow growth, thereby enhancing the precision of resistance detection. These refinements are supported by previous studies that emphasized improved test accuracy with a lower GC inoculum and extended incubation (Morlock et al., 2017; Mustazzolu et al., 2017, 2019; Piersimoni et al., 2013; Zhang et al., 2002).

The main genetic mechanism of PZA resistance lies in the mutations within the *pncA* gene, as evidenced by various studies which have reported 72 - 98 % of PZA resistance is attributed to *pncA* mutations (Che et al., 2021; Li et al., 2021; Shi et al., 2022). Contrarily, our study identified that only 45 % (14/31) of PZA resistance was contributed by *pncA* mutations. Other 41.9 % (13/31) of PZA resistance were due to alternative mechanisms without *pncA* mutations, and the remaining 12.9 % (4/31) of the resistance is still unknown. Moreover, in the case of MDR-TB isolates, resistance was predominantly linked to *pncA* mutations (32.2 %), with alternative mechanisms contributing to a lesser extent (6.4 %), consistent with previous findings (Khan et al., 2018; Whitfield et al., 2015).

The alternative mechanisms identified in our study were attributed to *panD* (9.6 %), *mas* (12.9 %), *glpK* (3.2 %), and *lprG* (3.2 %). Similarly, other studies have reported mutations in the alternative mechanisms such as *rpsA* (5.7 % to 72 %), *panD* (0.9 % to 2.5 %), *Rv2783c* (1.1 %), *Rv2044c* (0.74 %) (Akhmetova et al., 2015; Hameed et al., 2020; Liu et al., 2018; Shi et al., 2020; Tan et al., 2014; Werngren et al., 2017), *ClpC1, lprG, mas, gpsI*, and *fadD2* (Gopal et al., 2019; Lamont et al., 2020; Shi et al., 2018). Furthermore, we identified genes involved in efflux mechanisms associated with PZA resistance, such as *Rv1258c* (3.2 %), *Rv0191c* (3.2 %), and *Rv3008* (6.45 %), which is consistent with the results of Zhang et al. (2017) (Zhang et al., 2017). Among the alternative genes, *panD* is particularly noteworthy due to its established mechanistic role in PZA resistance. Prior studies have shown that pyrazinamide and its active form, POA, stimulate *panD* degradation by the ClpC1-ClpP protease system in *M. tuberculosis*. Mutations in *panD* may interfere with this degradation process, thereby conferring resistance and lending credibility to the *panD* mutations identified in our dataset. Interestingly, the mutation in the *glpk* gene identified in out resistant isolates have not been previously reported in clinical samples. However, these mutations have been previously described *in vitro* generated POA-resistant mutants by Gopal et al. (2016). The recurrence of this mutation in both *in vitro* and clinical isolate suggests selective advantage under drug pressure. These observations highlight the fact that Wayne's assay, though reporting >90 % sensitivity and specificity (Akhmetova et al., 2015), primarily detects *pncA* based resistance. Notably, one isolate identified as susceptible by Wayne's assay was found to be resistant to the SD MGIT DST with a mutation in the *pncA* gene, as confirmed by sequencing methods (Tables 1 **and** 2). The contradictory phenotypic results of 18 PZA-resistant isolates between Wayne's and SD MGIT DST, 14 were resolved by WGS analysis, and the remaining four isolates were still unclear, which might signify the limitation of the SD MGIT DST method employed in this study.

The identification of *glpK, mas,* and *lprG* mutations in clinical isolates in this study provides new insights into the genetic basis of PZA resistance. Previous studies have described mutations in these genes *in vitro* induced resistant strains, but not in any of the clinical strains (Gopal et al., 2016; Shi et al., 2018). Our findings address this gap by demonstrating the presence of these mutations in clinical isolates, indicating that experimentally identified resistance mechanisms may be clinically significant. The lack of these mutations in phenotypically sensitive isolates within our dataset further supports their potential role in resistance. Moreover, owing to the fact that the susceptible isolates in our dataset was limited, we made use of the susceptible isolates from the data of the previous study on South Indian isolates (Shanmugam et al., 2022). Although these genes may not be involved in the direct conversion of PZA to its active form POA, they might possess alternate mechanisms that affect PZA activity, which need to be explored. For instance, the *glpK* gene encodes glycerol kinase, which is involved in the central carbon metabolism in *M. tuberculosis*. Its disruption can reduce cellular energy and acidic intracellular state required for optimal PZA activity. Frameshift mutations in the *glpK* have led to the reduced efficacy of TB drugs and decreased the impact of PZA and a multidrug regimen containing PZA in animal models. Hence, it has been used as a specific marker for MDR-TB isolates (Bellerose et al., 2019). Phase variation in *glpK* occurs through reversible frameshift mutations in the homopolymeric region, which are linked to drug resistance, resulting in small colonies with heritable multidrug tolerance in *M. tuberculosis* (Safi et al., 2019).

The *mas* gene (mycocerosic acid synthase) regulates the synthesis of dimycocerosyl phthiocerol (DIM), a pathogenicity factor in *M. tuberculosis* (Sirakova et al., 2002). Disruption of this gene alters the lipid composition of the bacterial cell envelope, which may interfere with POA uptake or retention and has been shown to confer PZA resistance independent of *pncA* mutations (Gopal et al., 2016). *Mycobacterium tuberculosis* invades macrophages and modulates the host response through DIM. Mutations in DIM-synthesis genes, such as mas, can enhance *M. tuberculosis* pathogenicity, suggesting that DIM synthesis can be targeted for new antimycobacterial drugs (Augenstreich et al., 2020).

Similarly, *lprG* gene encodes a lipoprotein involved in the transport of triacylglycerides (TAGs) across the cell membrane and plays a crucial

role in maintaining lipid homeostasis in *M. tuberculosis* (Martinot et al., 2016) . Mutations in this gene have been shown to disrupt this transport mechanism, leading to intracellular accumulation of TAGs, which is associated with a drug-tolerant phenotype, potentially contributing to PZA resistance (Gopal et al., 2019). This accumulation may interfere with the susceptibility of the bacteria to PZA, highlighting the potential contribution of *lprG* disruption to PZA resistance. Additionally, Shi et al. (2018) reported mutations in *lprG* gene related to resistance against POA and PZA in *M. tuberculosis*. These studies support our observation indicating that various mechanisms, beyond *pncA* mutations, may affect PZA resistance (Shi et al., 2018).

Although our findings indicated potential associations between *glpK, mas, lprG* mutations and PZA resistance, these results should be interpreted cautiously. Previous studies have also reported similar candidate genes like *Rv0521, Rv3630, Rv2783, Rv0191, Rv3756c, Rv3008,* and *Rv1667c,* which are yet to be validated and their clinical significance is yet to be determined (Hameed et al., 2020; Shi et al., 2018; Zhang et al., 2017). Initially, *rpsA* was considered a key determinant of PZA resistance, but subsequent research refuted the proposed mechanism involving trans-translation, leading to the dismissal of the role of *rpsA* mutations in PZA resistance (Dillon et al., 2017). These examples highlight the need for caution when interpreting novel mutations, particularly in the absence of strong phenotypic correlation. Phenotypic drug susceptibility testing remains an essential method for validating drug resistance, particularly when new or rare genetic variants are encountered.

The discordance observed between phenotypic PZA resistance and *pncA* mutation status highlights the key diagnostic challenges. Several isolates exhibited phenotypic resistance despite the absence of *pncA* mutations, suggesting that other genetic determinants such as mutations in *panD, mas, glpK*, and *lprG* may underlie resistance. Conversely, some *pncA* mutations occurred in phenotypically susceptible isolates, suggesting the presence of neutral variants that do not confer resistance. These discrepancies underscore the limitations of relying solely on *pncA*-based molecular diagnostics.

To enhance diagnostic precision, it is crucial to identify region-specific resistance mutations and integrate them into existing molecular assays or genotypic DST, which currently examine only a few known mutations. Since PZA resistance may involve genes beyond *pncA*, WGS can also be employed to detect additional mutations. This method ensures consistency in testing processes, making the results more comparable and practical for routine use in TB diagnosis. Our findings support the integration of robust phenotypic methods, like the SD MGIT DST, alongside broader genotypic screening, to improve the accuracy of PZA resistance detection in clinical settings.

Despite these strengths, this study had several limitations that warrant consideration. First, the clinical isolates used in this study were retrieved from previously stored cultures confined to a particular geographic area of South Indian isolates, limiting the generalizability of our findings to a broader TB population. Much larger samples with a wider geographical setting may provide more insight into the PZA resistance mechanism. Second, while WGS facilitated the identification of novel mutations in genes such as *mas, glpK*, and *lprG*, functional validation assays like gene knockout or complementation experiments are required to elucidate the biological relevance of these variants and confirm their direct contribution to PZA resistance. Lastly, we identified phenotypically resistant isolates without any genotypic correlation, indicating that the SD MGIT DST method may yield false-resistant results at a lower percentage or they may exist other unknown mechanisms towards PZA resistance. These limitations highlight the need for integrated diagnostic approaches that combine refined phenotypic testing and comprehensive genomic analysis for accurate resistance detection.

5. Conclusion

This study demonstrates that the SD MGIT DST method offers a more accurate and reproducible approach for detecting PZA resistance in *M. tuberculosis* compared to conventional phenotypic methods. By significantly reducing false resistance rates and enabling a greater concordance with genotypic findings, the SD MGIT DST method enhances the reliability of PZA susceptibility testing. This method can be implemented with ease in any routine mycobacteriology laboratory, as it requires only a minimal procedural modification compatible with the standard MGIT 960 protocol, with no additional equipment or costs. Further validation in larger, multicentre studies will be essential to confirm its broader applicability and impact on effective TB treatment.

Funding sources

This study was funded by the Indian Council of Medical Research – Senior Research Fellowship (ICMR-SRF Grant ID: 2017-2590) and supported by an intramural research program at ICMR- National Institute for Research in Tuberculosis (ICMR-NIRT), India. KP is the recipient of a National Institutes of Health (NIH) R01 grant (Grant ID: 1R01AI170753–01A1), and AKR receives salary support from this grant.

Institutional review board statement

The protocols applied in this study were approved by the Ethics Committee of the ICMR-National Institute for Research in Tuberculosis (ICMR-NIRT), India, with the assigned NIRT-IEC ID 2019,002. All participants provided informed consent, and the results were not linked back to individual patients.

Credit author statement

Ananthi Rajendran: Data curation, Methodology, Formal analysis, Investigation, Visualization, Writing – original draft, Writing – review & editing. **Ahmed Kabir Refaya**: Data curation, Formal analysis, Visualization, Writing – review & editing. **Balaji Subramanyam**: Conceptualization, Methodology, Visualization. **Ramesh Karunaianantham**: Data curation, Methodology. **Dhandapani RaviKumar**: Methodology. **Hemalatha Haribabu**: Methodology. **Radha Gopalaswamy**: Data curation, Visualization. **Radhika Golla**: Methodology. **Vadivel Senthildevi**: Methodlogy. **Narayanan Sivaramakrishnan Gomathi**: Conceptualization. **Sivakumar Shanmugam**: Resources. **Kannan Palaniyandi**: Conceptualization, Formal analysis, Investigation, Funding acquisition, Project administration, Resources, Supervision, Writing – review & editing. The final version of the manuscript was reviewed and approved by all.

Declaration of competing interest

The authors declare that the research was conducted in the absence of commercial or financial relationships that could be construed as a potential conflict of interest.

Acknowledgements

The authors would like to thank the Director of the ICMR-National Institute for Research in Tuberculosis for facilitating this study. Furthermore, the invaluable experimental assistance provided department of bacteriology is duly acknowledged. Ananthi Rajendran acknowledges ICMR for SRF fellowship.

Supplementary materials

Supplementary material associated with this article can be found, in the online version, at doi:10.1016/j.crmicr.2025.100462.

Data availability

Whole-genome sequence data for the tuberculosis isolate reported in this study were deposited in NCBI (BioProject ID - PRJNA1097827, https://www.ncbi.nlm.nih.gov/search/all/?term=PRJNA1097827).

References

Ahmad, N., Ahuja, S.D., Akkerman, O.W., Alffenaar, J.-W.C., Anderson, L.F., Baghaei, P., Bang, D., Barry, P.M., Bastos, M.L., Behera, D., Benedetti, A., Bisson, G.P., Boeree, M. J., Bonnet, M., Brode, S.K., Brust, J.C.M., Cai, Y., Caumes, E., Cegielski, J.P., Menzies, D., 2018. Treatment correlates of successful outcomes in pulmonary multidrug-resistant tuberculosis: an individual patient data meta-analysis. Lancet 392 (10150), 821–834. https://doi.org/10.1016/S0140-6736(18)31644-1.

Akhmetova, Kozhamkulov, U., Bismilda, V., Chingissova, L., Abildaev, T., Dymova, M., Filipenko, M., Ramanculov, E., 2015. Mutations in the *pncA* and *rpsA* genes among 77 *Mycobacterium tuberculosis* isolates in Kazakhstan. Int. J. Tuberc. Lung Dis. 19 (2), 179–184. https://doi.org/10.5588/ijtld.14.0305.

Allix-Béguec, C., Arandjelovic, I., Bi, L., Beckert, P., Bonnet, M., Bradley, P., Cabibbe, A. M., Cancino-Muñoz, I., Caulfield, M.J., Chaiprasert, A., Cirillo, D.M., Clifton, D.A., Comas, I., Crook, D.W., De Filippo, M.R., de Neeling, H., Diel, R., Drobniewski, F.A., Faksri, K., Zhu, B., 2018. Prediction of susceptibility to first-line tuberculosis drugs by DNA sequencing. N. Engl. J. Med. 379 (15), 1403–1415. https://doi.org/10.1056/NEJMoa1800474.

Augenstreich, J., Haanappel, E., Sayes, F., Simeone, R., Guillet, V., Mazeres, S., Chalut, C., Mourey, L., Brosch, R., Guilhot, C., Astarie-Dequeker, C., 2020. Phthiocerol dimycocerosates from *Mycobacterium tuberculosis* increase the membrane activity of bacterial effectors and host receptors. Front. Cell Infect. Microbiol. 10. https://doi.org/10.3389/fcimb.2020.00420.

Balay, G., Abdella, K., Kebede, W., Tadesse, M., Bonsa, Z., Mekonnen, M., Amare, M., Abebe, G., 2024. Resistance to pyrazinamide in *Mycobacterium tuberculosis* complex isolates from previously treated tuberculosis cases in Southwestern Oromia, Ethiopia. J. Clin. Tuberc. Other Mycobact. Dis. 34. https://doi.org/10.1016/j.jctube.2023.100411.

Bellerose, M.M., Baek, S.H., Huang, C.C., Moss, C.E., Koh, E.I., Proulx, M.K., Smith, C.M., Baker, R.E., Lee, J.S., Eum, S., Shin, S.J., Cho, S.N., Murray, M., Sassetti, C.M., 2019. Common variants in the glycerol kinase gene reduce tuberculosis drug efficacy. mBio 10 (4). https://doi.org/10.1128/mBio.00663-19.

Bespiatykh, D., Bespyatykh, J., Mokrousov, I., Shitikov, E., 2021. A Comprehensive map of *Mycobacterium tuberculosis* complex regions of difference. mSphere 6 (4). https://doi.org/10.1128/msphere.00535-21.

Brudey, K., Driscoll, J.R., Rigouts, L., Prodinger, W.M., Gori, A., Al-Hajoj, S.A., Allix, C., Aristimuño, L., Arora, J., Baumanis, V., Binder, L., Cafrune, P., Cataldi, A., Cheong, S., Diel, R., Ellermeier, C., Evans, J.T., Fauville-Dufaux, M., Ferdinand, S., Sola, C., 2006. *Mycobacterium tuberculosis* complex genetic diversity: mining the fourth international spoligotyping database (SpolDB4) for classification, population genetics and epidemiology. BMC Microbiol. 6. https://doi.org/10.1186/1471-2180-6-23.

Brust, J.C.M., Shah, N.S., Gandhi, N.R., 2016. More on treatment outcomes in multidrug-resistant tuberculosis. N. Engl. J. Med. 375 (26). https://doi.org/10.1056/nejmc1613123.

Chang, K.C., Yew, W.W., Zhang, Y., 2011. Pyrazinamide susceptibility testing in mycobacterium tuberculosis: a systematic review with meta-analyses. Antimicrob. Agents Chemother. 55 (10), 4499–4505. https://doi.org/10.1128/AAC.00630-11.

Che, Y., Bo, D., Lin, X., Chen, T., He, T., Lin, Y., 2021. Phenotypic and molecular characterization of pyrazinamide resistance among multidrug-resistant *Mycobacterium tuberculosis* isolates in Ningbo, China. BMC Infect. Dis. 21 (1), 1–8. https://doi.org/10.1186/s12879-021-06306-1.

Demay, C., Liens, B., Burguière, T., Hill, V., Couvin, D., Millet, J., Mokrousov, I., Sola, C., Zozio, T., Rastogi, N., 2012. SITVITWEB - A publicly available international multimarker database for studying *Mycobacterium tuberculosis* genetic diversity and molecular epidemiology. Infect. Genet. Evol. 12 (4). https://doi.org/10.1016/j.meegid.2012.02.004.

Den Hertog, A.L., Menting, S., Pfeltz, R., Warns, M., Siddiqi, S.H., Anthony, R.M, 2016. Pyrazinamide is active against *Mycobacterium tuberculosis* cultures at neutral pH and low temperature. Antimicrob. Agents Chemother. 60 (8). https://doi.org/10.1128/AAC.00654-16.

Dillon, N.A., Peterson, N.D., Feaga, H.A., Keiler, K.C., Baughn, A.D., 2017. Anti-tubercular activity of pyrazinamide is independent of trans-translation and *rpsA*. Sci. Rep. 7 (1), 1–8. https://doi.org/10.1038/s41598-017-06415-5.

Driscoll, J.R., 2009. Spoligotyping for molecular epidemiology of the *Mycobacterium tuberculosis* complex. Methods Mol. Biol. 551, 117–128. https://doi.org/10.1007/978-1-60327-999-4_10.

Faksri, K., Xia, E., Tan, J.H., Teo, Y.Y., Ong, R.T.H., 2016. In silico region of difference (RD) analysis of *Mycobacterium tuberculosis* complex from sequence reads using RD-Analyzer. BMC Genom. 17 (1). https://doi.org/10.1186/s12864-016-3213-1.

Gopal, P., Grüber, G., Dartois, V., Dick, T., 2019. Pharmacological and molecular mechanisms behind the sterilizing activity of pyrazinamide. Trends Pharmaco. Sci. 40 (12), 930–940. https://doi.org/10.1016/j.tips.2019.10.005. Elsevier Ltd.

Gopal, P., Yee, M., Sarathy, J., Liang Low, J., Sarathy, J.P., Kaya, F., Dartois, V., Gengenbacher, M., Dick, T., 2016. Pyrazinamide resistance is caused by two distinct mechanisms: prevention of coenzyme a depletion and loss of virulence factor synthesis. ACS Infect. Dis. 2 (9), 616–626. https://doi.org/10.1021/acsinfecdis.6b00070.

Gouzy, A., Healy, C., Black, K.A., Rhee, K.Y., Ehrt, S., 2021. Growth of *Mycobacterium tuberculosis* at acidic pH depends on lipid assimilation and is accompanied by reduced GAPDH activity. Proc. Natl. Acad. Sci. U.S.A. 118 (32). https://doi.org/10.1073/pnas.2024571118.

Hameed, H.M.A., Tan, Y., Islam, M.M., Lu, Z., Chhotaray, C., Wang, S., Liu, Z., Fang, C., Tan, S., Yew, W.W., Zhong, N., Liu, J., Zhang, T., 2020. Detection of novel gene mutations associated with pyrazinamide resistance in multidrug-resistant *Mycobacterium tuberculosis* clinical isolates in Southern China. Infect. Drug Resist. 13, 217–227. https://doi.org/10.2147/IDR.S230774.

India TB Report, 2016. India TB Report 2016. TB India 2016 by RNTCP annual Report. https://tbcindia.mohfw.gov.in/wp-content/uploads/2023/05/4187947827National-Anti-TB-Drug-Resistance-Survey.pdf.

Indian mutation catalogue. (2022). *Indian catalogue of Mycobacterium tuberculosis mutations and their association with drug resistance-2022*. https://www.nirt.res.in/pdf/Indian%20Mutation%20Catalogue%202022.pdf.

Karmakar, M., Rodrigues, C.H.M., Horan, K., Denholm, J.T., Ascher, D.B., 2020. Structure guided prediction of Pyrazinamide resistance mutations in *pncA*. Sci. Rep. 10 (1), 1–10. https://doi.org/10.1038/s41598-020-58635-x.

Khan, M.T., Malik, S., Ali, S., Masood, N., Nadeem, T., Khan, A., & Afzal, M. (2019). Pyrazinamide resistance and mutations in *pncA* among isolates of *Mycobacterium tuberculosis* from Khyber Pakhtunkhwa, Pakistan. https://doi.org/10.1186/s12879-019-3764-2.

Khan, M.T., Malik, S.I., Ali, S., Sheed Khan, A., Nadeem, T., Zeb, M.T., Masood, N., Afzal, M.T., 2018. Prevalence of pyrazinamide resistance in Khyber Pakhtunkhwa, Pakistan. Microb. Drug Resist. 24 (9). https://doi.org/10.1089/mdr.2017.0234.

Köser, C.U., Ellington, M.J., Cartwright, E.J.P., Gillespie, S.H., Brown, N.M., Farrington, M., Holden, M.T.G., Dougan, G., Bentley, S.D., Parkhill, J., Peacock, S.J., 2012. Routine use of microbial whole genome sequencing in diagnostic and public health microbiology. PLoS Pathog. 8 (8). https://doi.org/10.1371/journal.ppat.1002824.

Kumar, A.K.H., Kadam, A., Karunaiaanantham, R., Tamizhselvan, M., Padmapriyadarsini, C., Mohan, A., Jeyadeepa, B., Radhakrishnan, A., Singh, U.B., Bapat, S., Mane, A., Kumar, P., Mamulwar, M., Bhavani, P.K., Haribabu, H., Rath, N., Guleria, R., Khan, A.M., Menon, J., 2024. Effect of metformin on plasma exposure of rifampicin, isoniazid, and pyrazinamide in patients on treatment for pulmonary tuberculosis. Ther. Drug Monit. 46 (3). https://doi.org/10.1097/FTD.0000000000001149.

Lamont, E.A., Dillon, N.A., Baughn, A.D., 2020. The bewildering antitubercular action of pyrazinamide. Microbiol. Mol. Biol. Rev. 84 (2), 1–15. https://doi.org/10.1128/mmbr.00070-19.

Letunic, I., Bork, P., 2021. Interactive tree of life (iTOL) v5: an online tool for phylogenetic tree display and annotation. Nucleic. Acids. Res. 49 (W1). https://doi.org/10.1093/nar/gkab301.

Li, K., Yang, Z., Gu, J., Luo, M., Deng, J., Chen, Y., 2021. Characterization of *pncA* mutations and prediction of PZA resistance in *Mycobacterium tuberculosis* clinical isolates from Chongqing, China. Front. Microbiol. 11 (January), 1–10. https://doi.org/10.3389/fmicb.2020.594171.

Liu, J., Shi, W., Zhang, S., Hao, X., Maslov, D.A., Shur, K.V., Bekker, O.B., Danilenko, V. N., Zhang, Y., 2019. Mutations in efflux pump Rv1258c (Tap) cause resistance to pyrazinamide, isoniazid, and streptomycin in *Mycobacterium tuberculosis*. Front. Microbiol. 10 (FEB). https://doi.org/10.3389/fmicb.2019.00216.

Liu, W., Chen, J., Shen, Y., Jin, J., Wu, J., Sun, F., Wu, Y., Xie, L., Zhang, Y., Zhang, W., 2018. Phenotypic and genotypic characterization of pyrazinamide resistance among multidrug-resistant *Mycobacterium tuberculosis* clinical isolates in Hangzhou, China. Clin. Microbiol. Infect. 24 (9), 1016.e1–1016.e5. https://doi.org/10.1016/j.cmi.2017.12.012.

Lv, H., Zhang, X., Zhang, X., Bai, J., You, S., Li, X., Li, S., Wang, Y., Zhang, W., Xu, Y., 2024. Global prevalence and burden of multidrug-resistant tuberculosis from 1990 to 2019. BMC Infect. Dis. 24 (1). https://doi.org/10.1186/s12879-024-09079-5.

Maharaj, K., 2016. Identification of *Mycobacterium tuberculosis pncA* gene single nucleotide polymorphisms conferring resistance to pyrazinamide. https://researchspace.ukzn.ac.za/server/api/core/bitstreams/88272df3-5737-4847-a1fd-d0a1d29a5429/content.

Martinot, A.J., Farrow, M., Bai, L., Layre, E., Cheng, T.Y., Tsai, J.H., Iqbal, J., Annand, J. W., Sullivan, Z.A., Hussain, M.M., Sacchettini, J., Moody, D.B., Seeliger, J.C., Rubin, E.J., 2016a. Mycobacterial metabolic syndrome: *lprG* and Rv1410 regulate triacylglyceride levels, growth rate and virulence in *Mycobacterium tuberculosis*. PLoS. Pathog. 12 (1). https://doi.org/10.1371/journal.ppat.1005351.

Miotto, P., Cabibbe, A.M., Feuerriegel, S., Casali, N., Drobniewski, F., Rodionova, Y., Bakonyte, D., Stakenas, P., Pimkina, E., Augustynowicz-Kopeć, E., Degano, M., Ambrosi, A., Hoffner, S., Mansjö, M., Werngren, J., Rüsch-Gerdes, S., Niemann, S., Cirillo, D.M., 2014. *Mycobacterium tuberculosis* pyrazinamide resistance determinants: a multicenter study. mBio 5 (5), 1–10. https://doi.org/10.1128/mBio.01819-14.

Mitchison, D.A., 1985. The action of antituberculosis drugs in short-course chemotherapy. Tubercle 66 (3), 219–225. https://doi.org/10.1016/0041-3879(85)90040-6.

Modlin, S.J., Marbach, T., Werngren, J., Mansjö, M., Hoffner, S.E., Valafar, F., 2021. Atypical genetic basis of pyrazinamide resistance in monoresistant mycobacterium tuberculosis. Antimicrob. Agents Chemother. 65 (6). https://doi.org/10.1128/AAC.01916-20.

Morlock, G.P., Tyrrell, F.C., Baynham, D., Escuyer, V.E., Green, N., Kim, Y., Longley-Olson, P.A., Parrish, N., Pennington, C., Tan, D., Austin, B., Posey, J.E., 2017. Using reduced inoculum densities of *Mycobacterium tuberculosis* in MGIT pyrazinamide susceptibility testing to prevent false-resistant results and improve accuracy: a

multicenter evaluation. Tuberc. Res. Treat. 2017, 1–9. https://doi.org/10.1155/2017/3748163.
Mustazzolu, A., Iacobino, A., Giannoni, F., Piersimoni, C., Fattorini, L., the Italian Multicentre Study on Resistance to Antituberculosis Drugs (SMIRA) Group, 2017. Improved bactec MGIT 960 pyrazinamide test decreases detection of false *Mycobacterium tuberculosis* pyrazinamide resistance. J. Clin. Microbiol. 55 (12), 3552–3553. https://doi.org/10.1128/JCM.01437-17.
Mustazzolu, A., Piersimoni, C., Iacobino, A., Giannoni, F., Chirullo, B., Fattorini, L., 2019. Revisiting problems and solutions to decrease *Mycobacterium tuberculosis* pyrazinamide false resistance when using the Bactec MGIT 960 system. Ann. Dell'Istituto Super. Sanita 55 (1). https://doi.org/10.4415/ANN_19_01_09.
Nasiri, M.J., Fardsanei, F., Arshadi, M., Deihim, B., Khalili, F., Dadashi, M., Goudarzi, M., Mirsaeidi, M., 2021. Performance of Wayne assay for detection of pyrazinamide resistance in *Mycobacterium tuberculosis*: a meta-analysis study. New. Microbes. New. Infect. 42. https://doi.org/10.1016/j.nmni.2021.100886.
Nimmo, C., Shaw, L.P., Doyle, R., Williams, R., Brien, K., Burgess, C., Breuer, J., Balloux, F., Pym, A.S., 2019. Whole genome sequencing *Mycobacterium tuberculosis* directly from sputum identifies more genetic diversity than sequencing from culture. BMC Genom. 20 (1). https://doi.org/10.1186/s12864-019-5782-2.
Peterson, N.D., Rosen, B.C., Dillon, N.A., Baughn, A.D., 2015. Uncoupling environmental pH and intrabacterial acidification from pyrazinamide susceptibility in *Mycobacterium tuberculosis*. Antimicrob. Agents Chemother. 59 (12). https://doi.org/10.1128/AAC.00967-15.
Phelan, J.E., O'Sullivan, D.M., Machado, D., Ramos, J., Oppong, Y.E.A., Campino, S., O'Grady, J., McNerney, R., Hibberd, M.L., Viveiros, M., Huggett, J.F., Clark, T.G., 2019. Integrating informatics tools and portable sequencing technology for rapid detection of resistance to anti-tuberculous drugs. Genome Med. 11 (1). https://doi.org/10.1186/s13073-019-0650-x.
Piddington, D.L., Kashkouli, A., Buchmeier, N.A., 2000. Growth of *Mycobacterium tuberculosis* in a defined medium is very restricted by acid pH and Mg2+ levels. Infect. Immun. 68 (8). https://doi.org/10.1128/IAI.68.8.4518-4522.2000.
Piersimoni, C., Mustazzolu, A., Giannoni, F., Bornigia, S., Gherardi, G., Fattorini, L., 2013. Prevention of false resistance results obtained in testing the susceptibility of *Mycobacterium tuberculosis* to pyrazinamide with the bactec MGIT 960 system using a reduced inoculum. J. Clin. Microbiol. 51 (1):, 291–294. https://doi.org/10.1128/JCM.01838-12.
PMDT guidelines, 2021. Guidelines for Programmatic Management of Drug-resistant TB in India. 8368587497Guidelines-for-PMDT-in-India-1.
Pullan, S.T., Allnutt, J.C., Devine, R., Hatch, K.A., Jeeves, R.E., Hendon-Dunn, C.L., Marsh, P.D., Bacon, J., 2016. The effect of growth rate on pyrazinamide activity in *Mycobacterium tuberculosis* - insights for early bactericidal activity? BMC Infect. Dis. 16 (1). https://doi.org/10.1186/s12879-016-1533-z.
Rajendran, A., Palaniyandi, K., 2022. Mutations associated with pyrazinamide resistance in mycobacterium tuberculosis: a review and update. In: Current Microbiology, 79. https://doi.org/10.1007/s00284-022-03032-y.
Ramirez-Busby, S.M., Rodwell, T.C., Fink, L., Catanzaro, D., Jackson, R.L., Pettigrove, M., Catanzaro, A., Valafar, F., 2017. A multinational analysis of mutations and heterogeneity in *PZase, RpsA,* and *PanD* associated with pyrazinamide resistance in M/XDR *Mycobacterium tuberculosis*. Sci. Rep. 7 (1), 1–9. https://doi.org/10.1038/s41598-017-03452-y.
Safi, H., Gopal, P., Lingaraju, S., Ma, S., Levine, C., Dartois, V., Yee, M., Li, L., Blanc, L., Liang, H.P.H., Husain, S., Hoque, M., Soteropoulos, P., Rustad, T., Sherman, D.R., Dick, T., Alland, D., 2019. Phase variation in *Mycobacterium tuberculosis glpK* produces transiently heritable drug tolerance. Proc. Natl. Acad. Sci. U.S.A 116 (39). https://doi.org/10.1073/pnas.1907631116.
Salfinger, M., Heifets, L.B., 1988. Determination of pyrazinamide MICs for *Mycobacterium tuberculosis* at different pHs by the radiometric method. Antimicrob. Agents Chemother. 32 (7), 1002–1004. https://doi.org/10.1128/AAC.32.7.1002.
Shanmugam, S.K., Kumar, N., Sembulingam, T., Ramalingam, S.B., Selvaraj, A., Rajendhiran, U., Solaiyappan, S., Tripathy, S.P., Natrajan, M., Chandrasekaran, P., Swaminathan, S., Parkhill, J., Peacock, S.J., Ranganathan, U.D.K., 2022. *Mycobacterium tuberculosis* lineages associated with mutations and drug resistance in isolates from India. Microbiol. Spectr. 10 (3). https://doi.org/10.1128/spectrum.01594-21.
Shaojun, P., Xichao, O., 2024. Interpretation of the World Health Organization's Catalogue of mutations in *Mycobacterium tuberculosis* complex and their association with drug resistance (2nd Edition). Chin. J. Antituberc. 46 (3). https://doi.org/10.19982/j.issn.1000-6621.20230450.
Sharma, B., Pal, N., Malhotra, B., Vyas, L., Rishi, S., 2010a. Comparison of MGIT 960 & pyrazinamidase activity assay for pyrazinamide susceptibility testing of *Mycobacterium tuberculosis*. Indian J. Med. Res. 132 (7), 72–76. https://pubmed.ncbi.nlm.nih.gov/20693593/.
Sharma, S., Kumar, M., Sharma, S., Nargotra, A., Koul, S., Khan, I.A., 2010b. Piperine as an inhibitor of Rv1258c, a putative multidrug efflux pump of Mycobacterium tuberculosis. J. Antimicrob. Chemother. 65 (8). https://doi.org/10.1093/jac/dkq186.
Shi, D., Zhou, Q., Xu, S., Zhu, Y., Li, H., Xu, Y., 2022. Pyrazinamide resistance and *pncA* mutation profiles in multidrug resistant mycobacterium tuberculosis. Infect. Drug Resist. 15. https://doi.org/10.2147/IDR.S368444.
Shi, Su, R., Zheng, D., Zhu, Y., Ma, X., Wang, S., Li, H., Sun, D., 2020. Pyrazinamide resistance and mutation patterns among multidrug-resistant *Mycobacterium tuberculosis* from Henan Province. Infect. Drug Resist. 13, 2929–2941. https://doi.org/10.2147/IDR.S260161.
Shi, W., Chen, J., Zhang, S., Zhang, W., Zhang, Y., 2018. Identification of novel mutations in *lprG* (*rv1411c*), *rv0521, rv3630, rv0010c, ppsC*, and *cyp128* associated with pyrazinoic acid/pyrazinamide resistance in *Mycobacterium tuberculosis*. Antimicrob. Agents Chemother. 1–4. https://doi.org/10.1128/AAC.00430-18.
Siddiqi, S.H., Rüsch-Gerdes, S., 2006. For BACTEC™ MGIT 960™ TB System (Also applicable for Manual MGIT) Mycobacteria Growth Indicator Tube (MGIT) Culture and Drug Susceptibility Demonstration Projects. https://www.finddx.org/wp-content/uploads/2023/02/20061101_rep_mgit_manual_FV_EN.pdf.
Sirakova, T.D., Fitzmaurice, A.M., Kolattukudy, P., 2002. Regulation of expression of *mas* and *fadD28*, two genes involved in production of dimycocerosyl phthiocerol, a virulence factor of *Mycobacterium tuberculosis*. J. Bacteriol. 184 (24). https://doi.org/10.1128/JB.184.24.6796-6802.2002.
Somerville, W., Thibert, L., Schwartzman, K., Behr, M.A., 2005. Extraction of *Mycobacterium tuberculosis* DNA: a question of containment. J. Clin. Microbiol. 43 (6). https://doi.org/10.1128/JCM.43.6.2996-2997.2005.
Stoffels, K., Mathys, V., Fauville-Dufaux, M., Wintjens, R., Bifania, P., 2012. Systematic analysis of pyrazinamide-resistant spontaneous mutants and clinical isolates of *Mycobacterium tuberculosis*. Antimicrob. Agents Chemother. 56 (10), 5186–5193. https://doi.org/10.1128/AAC.05385-11.
Sun, Q., Li, X., Perez, L.M., Shi, W., Zhang, Y., Sacchettini, J.C., 2020. The molecular basis of pyrazinamide activity on *Mycobacterium tuberculosis panD*. Nat. Commun. 11 (1), 1–7. https://doi.org/10.1038/s41467-019-14238-3.
Tamilzhalagan, S., Justin, E.S., Selvaraj, A., Venkateswaran, K., Sivakumar, A.K., Chittibabu, S., McLaughlin, H.P., Moonan, P.K., Smith, J.P., Suba, S., Sathya Narayanan, M.K., Ho, C.S., Kumar, N., Tripathy, S.P., Shanmugam, S.K., Hall-Eidson, P.J., Ranganathan, U.D., 2025. Phenotypic and genotypic characterization of *Mycobacterium tuberculosis* pyrazinamide resistance—India, 2018–2020. Front. Microbiol. 15. https://doi.org/10.3389/fmicb.2024.1515627.
Tan, Y., Hu, Z., Zhang, T., Cai, X., Kuang, H., Liu, Y., Chen, J., Yang, F., Zhang, K., Tan, S., Zhao, Y., 2014. Role of *pncA* and *rpsA* gene sequencing in detection of pyrazinamide resistance in *Mycobacterium tuberculosis* isolates from southern China. J. Clin. Microbiol. 52 (1), 291–297. https://doi.org/10.1128/JCM.01903-13.
Thiede, J.M., Dillon, N.A., Howe, M.D., Aflakpui, R., Modlin, S.J., Hoffner, S.E., Valafar, F., Minato, Y., Baughn, A.D., 2021. Pyrazinamide action is driven by the cell envelope stress response in *Mycobacterium tuberculosis*. bioRxiv. https://doi.org/10.1128/mbio.00439-21.
Thuansuwan, W., Chuchottaworn, C., Nakajima, C., Suzuki, Y., Chaichanawongsaroj, N., 2024. Biphasic medium using nicotinamide for detection of pyrazinamide resistance in *Mycobacterium tuberculosis*. Antibiotics 13 (6). https://doi.org/10.3390/antibiotics13060563.
Ullah, I., Javaid, A., Tahir, Z., Ullah, O., Shah, A.A., Hasan, F., Ayub, N., 2016. Pattern of drug resistance and risk factors associated with development of drug-resistant *Mycobacterium tuberculosis* in Pakistan. PLoS One 11 (1). https://doi.org/10.1371/journal.pone.0147529.
Wang, Z., Tang, Z., Heidari, H., Molaeipour, L., Ghanavati, R., Kazemian, H., Koohsar, F., Kouhsari, E., 2023. Global status of phenotypic pyrazinamide resistance in *Mycobacterium tuberculosis* clinical isolates: an updated systematic review and meta-analysis. J. Chemother. 35 (7), 583–595. https://doi.org/10.1080/1120009X.2023.2214473. Taylor and Francis Ltd.
Shi, Wanliang, 2021. Activity of pyrazinamide against *Mycobacterium tuberculosis* at neutral pH in PZA-S1 minimal medium. Antibiotics 10 (8). https://doi.org/10.3390/antibiotics10080909.
Werngren, J., Alm, E., Mansjö, M., 2017. Non-*pncA* gene-mutated but pyrazinamide-resistant mycobacterium tuberculosis: why is that? J. Clin. Microbiol. 55 (6), 1920–1927. https://doi.org/10.1128/JCM.02532-16.
Werngren, J., Mansjö, M., Glader, M., Hoffner, S., Forsman, L.D., 2021. Detection of pyrazinamide heteroresistance in *Mycobacterium tuberculosis*. Antimicrob. Agents Chemother. 65 (9). https://doi.org/10.1128/AAC.00720-21.
Werngren, J., Sturegård, E., Juréen, P., Ängeby, K., Hoffner, S., Schönd, T., 2012. Reevaluation of the critical concentration for drug susceptibility testing of *Mycobacterium tuberculosis* against pyrazinamide using wild-type MIC distributions and *pncA* gene sequencing. Antimicrob. Agents Chemother. 56 (3), 1253–1257. https://doi.org/10.1128/AAC.05894-11.
Whitfield, Soeters, H.M., Warren, R.M., York, T., Sampson, S.L., Streicher, E.M., Van Helden, P.D., Van Rie, A., 2015. A global perspective on pyrazinamide resistance: systematic review and meta-analysis. PLoS One 10 (7), 1–16. https://doi.org/10.1371/journal.pone.0133869.
WHO, 2024. Global tuberculosis report. https://iris.who.int/bitstream/handle/10665/379339/9789240101531-eng.pdf?sequence=1.
WHO mutation catalogue, 2021. Catalogue of Mutations in *Mycobacterium tuberculosis* Complex and their Association with Drug Resistance. https://www.who.int/publications/i/item/9789240028173.
World Health Organization, 2018. Technical manual for drug susceptibility testing of medicines used in the treatment of tuberculosis Geneva: world Health Organization; 2018. Licence: CC BY-NC-SA 3.0 IGO. Guideline 6 (1). https://iris.who.int/bitstream/handle/10665/275469/9789241514842-eng.pdf?sequence=1.
Zhang, Y., Mitchison, D., 2003. The curious characteristics of pyrazinamide: a review. Int. J. Tuberc. Lung Dis. J. Int. Union Tuberc. Lung Dis 7 (1), 6–21. https://pubmed.ncbi.nlm.nih.gov/12701830/.
Zhang, Y., Permar, S., Sun, Z., 2002. Conditions that may affect the results of susceptibility testing of *Mycobacterium tuberculosis* to pyrazinamide. J. Med. Microbiol. 51 (1), 42–49. https://doi.org/10.1099/0022-1317-51-1-42.
Zhang, Y., Wade, M.M., Scorpio, A., Zhang, H., Sun, Z., 2003. Mode of action of pyrazinamide: disruption of *Mycobacterium tuberculosis* membrane transport and energetics by pyrazinoic acid. J. Antimicrob. Chemother. 52 (5), 790–795. https://doi.org/10.1093/jac/dkg446.
Zhang, Y., Zhang, J., Cui, P., Zhang, Y., Zhang, W., 2017. Identification of novel efflux proteins Rv0191, Rv3756c, Rv3008, and Rv1667c involved in pyrazinamide

resistance in *Mycobacterium tuberculosis*. Antimicrob. Agents Chemother. 61 (8). https://doi.org/10.1128/AAC.00940-17.